Russbach, Austria, March 9-15 2014

The Macroscopic-Microscopic Nuclear-Structure Model Foundations and Results

Peter Möller

Los Alamos

Collaborators on this and other projects:
W. D. Myers, J. Randrup(LBL), H. Sagawa (Aizu), S. Yoshida (Hosei), T. Ichikawa(YITP), A. J. Sierk(LANL), A. Iwamoto (JAEA), S. Aberg (Lund), R. Bengtsson (Lund), S. Gupta (IIT, Ropar), and many experimental groups (e. g. K.-L. Kratz (Mainz), H. Schatz (MSU), A. Andreyev (York) . . .).

More details about masses, other projects (beta-decay,fission), associated ASCII data files, interactive access to data (type in Z, A and get specific data, contour maps) and figures are at

http://t2.lanl.gov/nis/molleretal/

Global Nuclear-Structure Modeling

Historically success is associated with

- Relatively simple ideas
- Few model parameters
- Consistent application
- Close look at experimental data

What is a model?

- Can be explained(!)
- Can describe new data
- Can describe other types of quantities than those that primarily motivated its development
- Can be generalized to describe new stuff.

Bethe-Weizsäcker Mass Model (1935)

In the first global MACROSCOPIC nuclear-mass model the nuclear ground-state mass is given by

$$E_{\rm mac}^{\rm FL}(Z, N, {\rm shape}) =$$

$$\begin{array}{lr} M_{\rm H}Z & ({\rm Hydrogen-atom\ mass}) \\ +M_{\rm n}N & ({\rm Neutron\ mass}) \\ -B(N,Z) & ({\rm Nuclear\ binding\ energy}) \end{array}$$

Nuclear Binding Energy BW (1935)

The nuclear binding energy according to BW is given by

$$
\begin{aligned}
B(N,Z) = \\
& +a_{\mathrm{v}} A && \text{(Volume energy)} \\
& -a_{\mathrm{s}} A^{2/3} && \text{(Surface energy)} \\
& -a_{\mathrm{C}} \frac{Z^2}{A^{1/3}} && \text{(Coulomb energy)} \\
& -a_I \frac{(N-Z)^2}{A} && \text{(Symmetry energy)} \\
& -\delta(A) && \text{(Pairing energy)}
\end{aligned}
$$

Nuclear POTENTIAL ENERGY BW (1939)

$$B(N,Z) =$$

$$+a_{\mathrm{V}}A \qquad \text{(Volume energy)}$$

$$-a_{\mathrm{S}}A^{2/3}B_s(\beta) \qquad \text{(Surface energy)}$$

$$-a_{\mathrm{C}}\frac{Z^2}{A^{1/3}}B_C(\beta) \qquad \text{(Coulomb energy)}$$

$$-a_I\frac{(N-Z)^2}{A} \qquad \text{(Symmetry energy)}$$

$$-\delta(A) \qquad \text{(Pairing energy)}$$

Nuclear Deformation Energy

Let the nuclear surface be described by

$$r(\theta, \phi) = R_0 \left[1 + \alpha_2 P_2(\cos\theta)\right]$$

The surface energy lowest order Taylor expansion:

$$E_{\mathrm{s}} = E_{\mathrm{s}}^0 (1 + \frac{2}{5} {\alpha_2}^2)$$

The Coulomb energy lowest order Taylor expansion

$$E_{\mathrm{C}} = E_{\mathrm{C}}^0 (1 - \frac{1}{5} {\alpha_2}^2)$$

The energy at deformation α_2 relative to spherical shape

$$E_{\mathrm{def}}(\alpha_2) = E_{\mathrm{C}}(\alpha_2) + E_{\mathrm{s}}(\alpha_2) - (E_{\mathrm{C}}^0 + E_{\mathrm{s}}^0)$$

If E_{def} is negative then the system has no barrier wrt fission

$$E_{\mathrm{def}}(\alpha_2) = \frac{2}{5} {\alpha_2}^2 E_{\mathrm{s}}^0 - \frac{1}{5} {\alpha_2}^2 E_{\mathrm{C}}^0 < 0$$

$$1 < \frac{E_{\mathrm{C}}^0}{2E_{\mathrm{s}}^0} = x$$

The surface energy for a sphere

$$E_{\mathrm{s}}^{0} = 17.80 A^{2/3}$$

The Coulomb energy for a sphere

$$E_{\mathrm{C}}^{0} = 0.7103 \frac{Z^2}{A^{1/3}}$$

The fissility parameter x:

$$x = \frac{Z^2}{50.13 A}$$

Z	A	x
50	124	0.402
82	208	0.645
92	138	0.709
100	252	0.792
114	298	0.870
125	328	0.950
130	335	1.006

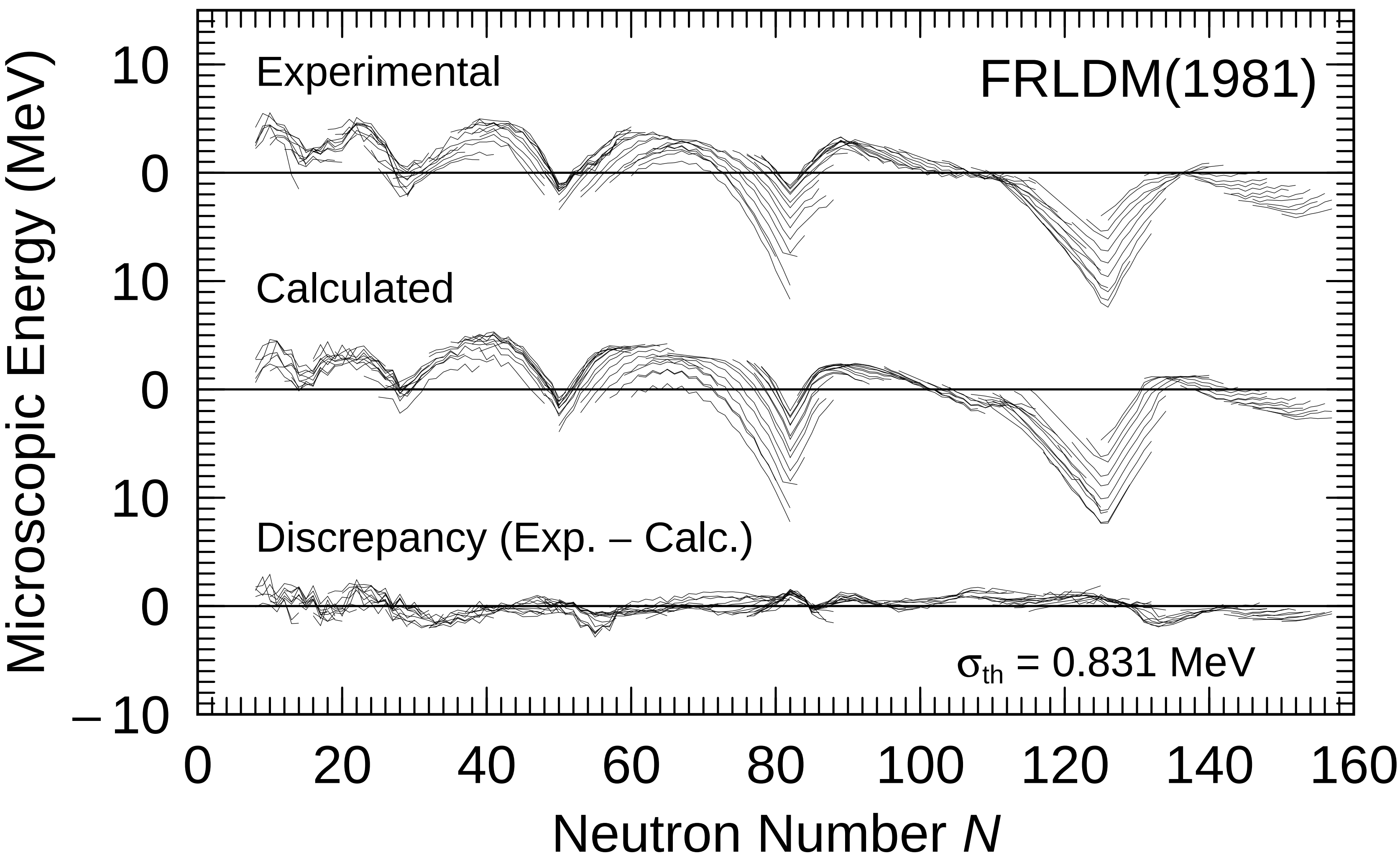
FRLDM(1981)
Experimental
Calculated
Discrepancy (Exp. – Calc.)
σth = 0.831 MeV
Microscopic Energy (MeV)
Neutron Number N
10
0
10
0
10
0
–10
0
20
40
60
80
100
120
140
160

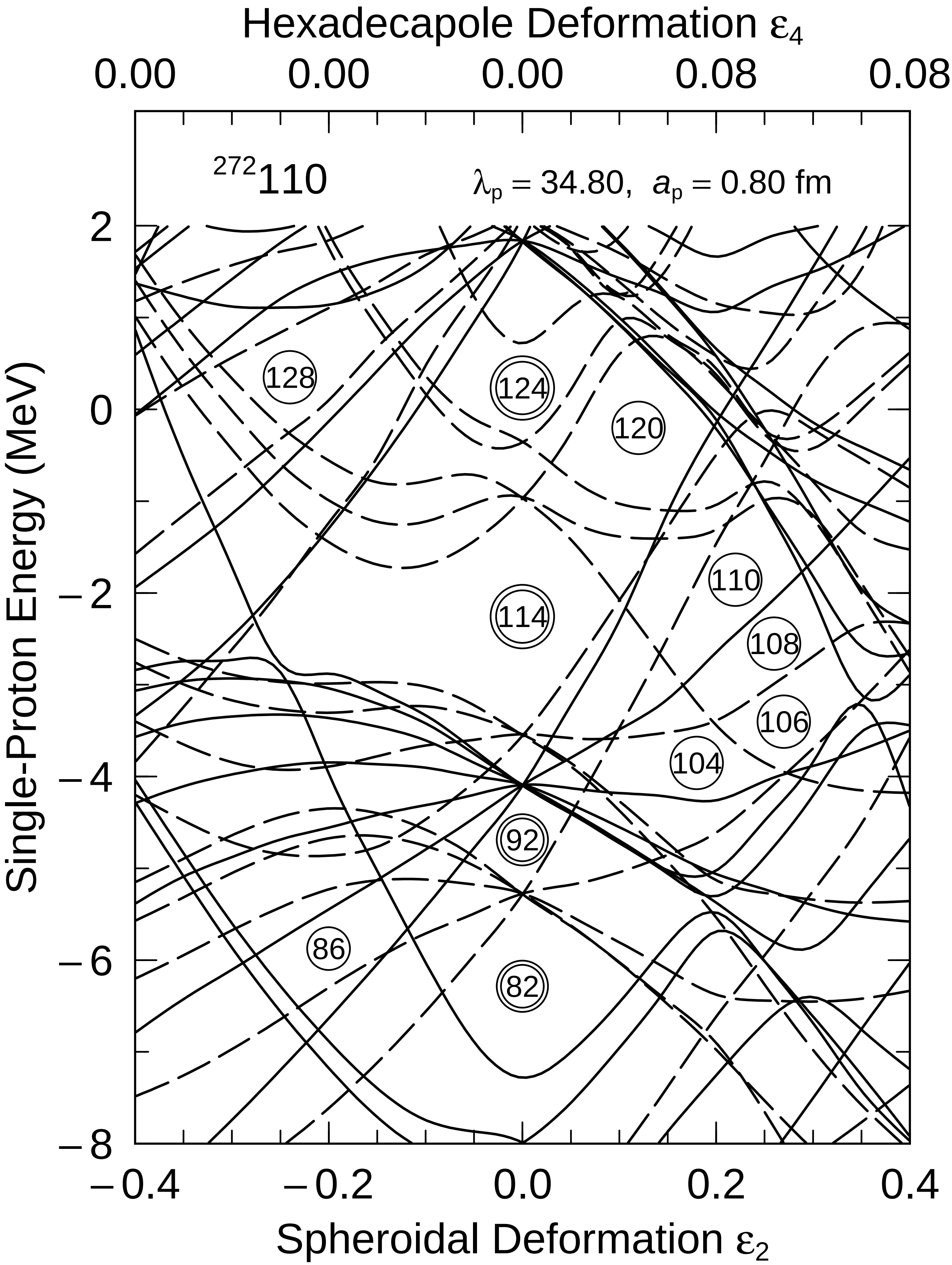

Hexadecapole Deformation ε4
0.00
0.00
0.00
0.08
0.08
272110
λp = 34.80, ap = 0.80 fm
128
124
120
114
110
108
106
104
92
86
82
2
0
−2
−4
−6
−8
Single-Proton Energy (MeV)
−0.4
−0.2
0.0
0.2
0.4
Spheroidal Deformation ε2

trend is consistent with a straight line, defining $(Z^2/A)_c = 40.2\pm0.7$. The equation of the line leads to the semiempirical formula,

$$M_2-M_1=0.090(40.2\pm0.7-Z^2/A)^{\frac{1}{2}}A. \quad (4)$$

One may combine Eq. (4) with the relation:

$$M_2+M_1=A-\nu$$
(ν=number of neutrons emitted in fission),

to predict the positions of the peaks in the yield curves of elements that have not yet been investigated. If an average value $\bar{\nu}=2.8$ is used, one finds

$$M_2=\tfrac{1}{2}A-1.4+0.045(40.2\pm0.7-Z^2/A)^{\frac{1}{2}}A, \quad (5)$$

$$M_1=\tfrac{1}{2}A-1.4-0.045(40.2\pm0.7-Z^2/A)^{\frac{1}{2}}A. \quad (6)$$

The present analysis provides a reason for the empirical observation that in the fission of different elements the position of the heavy peak remains approximately constant. If the degree of asymmetry remained unchanged from nucleus to nucleus, both peaks would move towards higher masses with increasing A. In fact, there is superimposed on this shift a coming together of the peaks with increasing Z^2/A. Since the over-all trend of Z^2/A is to increase with A, the result is that for the light peak the two shifts add up whereas for the heavy peak they partly cancel. This is illustrated in Table I, where M_2 and M_1, calculated according to (5) and (6), are compared with the observed values.

TABLE I. Positions of the peaks in the fission yield curves.

Compound nucleus	Position of peaks: Observed[a] M_2	M_1	Formulas (5), (6) M_2	M_1	Remarks	Reference
Th^{233}	140	91	139.1	91.1	Low-energy neutron fission	b
U^{239}	140	98	141.1	95.1		c
U^{236}	138.5	95	138.2	95.0		d
U^{234}	137	93	136.2	95.0		b, e
Pu^{240}	138	99	137.9	99.3		c
U^{238}	140	96	140.2	95.0	Spontaneous fission	f, g
Cm^{242}	136	103	134.7	104.5		g
Cf^{252}	139	108	140.2	109.0		h

[a] The uncertainty in the observed values of M_2 and M_1 is of the order of ±1 or ±2 mass units. (It is more in the cases of U^{239} and U^{238}.) No systematic attempt has been made to adjust $A-M_2-M_1$ to agree with available information on the number of emitted neutrons.
[b] A. Turkevich and J. B. Niday, Phys. Rev. **84**, 52 (1951).
[c] E. B. Steinberg and M. S. Freedman, *Radiochemical Studies: The Fission Products* (McGraw-Hill Book Company, Inc., New York, 1951). Paper No. 219, National Nuclear Energy Series, Plutonium Project Record, Vol. 9, Div. IV, Part V.
[d] Glendenin, Steinberg, Inghram, and Hess, Phys. Rev. **84**, 860 (1951).
[e] Steinberg, Glendenin, Inghram, and Hayden, Phys. Rev. **95**, 867 (1954).
[f] G. W. Wetherill, Phys. Rev. **92**, 907 (1953).
[g] E. P. Steinberg and L. E. Glendenin, Phys. Rev. **95**, 431 (1954).
[h] E. P. Steinberg and L. E. Glendenin, J. Inorg. Nuc. Chem. **1**, 45 (1955).

Further measurements of fission asymmetries would be interesting, especially in the region of Z^2/A close to the critical value, where the present considerations suggest a rapid decrease of M_2-M_1.

It is a pleasure to acknowledge stimulating discussions with Professor S. G. Thompson, Dr. A. C. Pappas, and Dr. T. Maris.

[1] N. Bohr and J. A. Wheeler, Phys. Rev. **56**, 426 (1939).
[2] A. E. S. Green, Phys. Rev. **95**, 1006 (1954).
[3] W. J. Swiatecki (to be published).
[4] D. L. Hill and J. A. Wheeler, Phys. Rev. **89**, 1102 (1953).

Systematics of Spontaneous Fission Half-Lives

W. J. SWIATECKI
Institute for Mechanics and Mathematical Physics and The Gustaf Werner Institute for Nuclear Chemistry, Uppsala, Sweden
(Received July 18, 1955)

SEVERAL authors have noted the over-all trend of spontaneous fission half-lives to decrease with increasing Z^2/A as well as the considerable deviations (by several powers of 10) from any smooth dependence on this parameter.[1] We should like to discuss the close correlation which seems to exist between the half-lives and the finer details in the systematics of the ground-state masses of nuclei.[2]

A simple way of exhibiting this correlation is to plot the deviation $\delta\tau$ from a straight line in a plot of $\tau[\tau=\log_{10}(\text{half-life})]$ *vs* Z^2/A, against deviations (δM) of the masses M of the nuclei from a smooth reference surface $M_{\text{ref}}(A,Z)$. We made such a plot, with M_{ref} taken to be the semiempirical mass surface of Green[3] (based on the liquid drop model):

$$\delta M=M-M_{\text{ref}},$$
$$M_{\text{ref}}=1000A-8.3557A+19.120A^{\frac{2}{3}}+0.76278Z^2/A^{\frac{1}{3}}+25.444(N-Z)^2/A+0.420(N-Z)\text{ millimass units.} \quad (1)$$

The experimental masses M were taken from Glass *et al.*[4]

In the case of even-even nuclei the plot of $\delta\tau$ *vs* δM suggested a series of straight lines, one for each Z, indicating that for the isotopes of one element special stability of a nucleus (small δM) is invariably associated with a longer lifetime (large $\delta\tau$). The lines had approximately the same slope, thus defining a spontaneous-fission hindrance factor which corresponds to about 10^5 times longer lifetime for each millimass unit of extra stability. This suggested that if the observed lifetimes were corrected for the variations in stability of the ground states, a more regular dependence of τ on Z^2/A might be discernible.

Figure 1 shows the effect on the plot of τ *vs* Z^2/A of adding to the observed τ_{exp} an empirical correction $k\delta M$ ($k\sim5$ if δM in mMU). For even-even nuclei the values of $\tau_{\text{exp}}+k\delta M$ define a fairly smooth curve, with indications of a similar curve for odd-A nuclei. [In a preliminary plot the hindrance factor k was taken to be 5. A small but significant further smoothing of the points resulted from making k vary with Z^2/A according to $k=5-(Z^2/A-37.5)$. This is the case shown in Fig. 1.]

The result can be stated in the form of an empirical formula for half-lives; e.g., for even-even nuclei,

$$\tau_{ee}=f(Z^2/A)-k\delta M, \tag{2}$$

where f is the curve defined by the even-even points in Fig. 1. The relation of the points for odd-A nuclei to the curve obtained from (2) by a shift upwards of 6.6 units is also shown in Fig. 1. The lifetime of the odd-odd nucleus E^{254} (einsteinium, $Z=99$) is consistent with a further shift of 4.9 units. The curve $f(Z^2/A)$ can be represented for example by a cubic, which leads to the following formulas for the lifetimes:

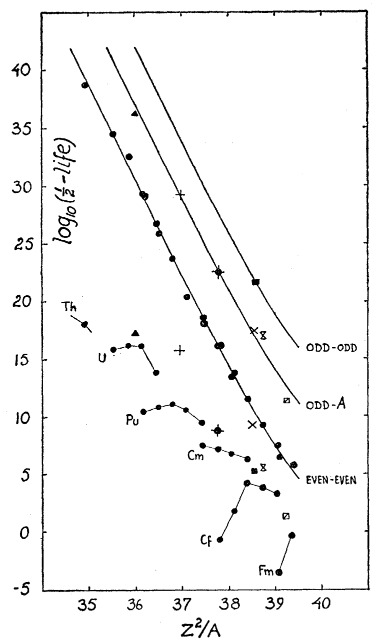

FIG. 1. Plot of spontaneous fission half-lives against Z^2/A. The observed lifetimes τ_{exp} occupy the bottom left-hand part of the figure; the "corrected" values $\tau_{\text{exp}}+k\delta M$ group themselves around the three curves. Experimental points for even-even nuclei are joined by straight lines. Odd-A nuclei are designated by special symbols which, reading from left to right along the odd-A curve, refer to U^{235}, Pu^{239}, Bk^{249}, Cf^{249}, E^{253} (einsteinium, $Z=99$), and Fm^{255} (fermium, $Z=100$). The odd-odd nucleus E^{254} is marked by a square.

$$\left.\begin{array}{r}\tau_{ee}=18.2\\ \tau_{\text{odd }A}=24.8\\ \tau_{oo}=29.7\end{array}\right\}-7.8\theta+0.35\theta^2+0.073\theta^3-(5-\theta)\delta M, \tag{3}$$

where $\theta=(Z^2/A)-37.5$, and δM is the deviation in mMU of the experimental mass from the surface (1). Table I compares the observed half-lives with the values calculated by means of (3). The remarkable degree of smoothing achieved by means of the unsophisticated correction $k\delta M$ is illustrated by the fact that the deviations from (3) rarely exceed 0.5. (Note that a shift in τ of this amount would be produced by an error of 0.1 mMU in δM.)

TABLE I. Values of $\log_{10}$(half-life).

Nucleus	Experimental[a]	Formula (3)	Nucleus	Experimental[a]	Formula (3)
Even-even nuclei			Even-even nuclei		
Th 230	≥7.18	19.39	Cf 246	3.32	3.27
232	18.15	18.84	248	3.85	3.92
U 232	13.90	13.56	250	4.18	4.24
234	16.30	15.98	252	1.82	1.60
236	16.30	15.21	254	−0.70	−1.02
238	15.90	15.52	Fm 254	−0.30	−0.85
Pu 236	9.54	9.66	256	−3.52	−3.02
238	10.69	11.57			
240	11.08	11.09	Odd-A nuclei		
242	10.86	11.22	U 235	17.26?	18.02
244	10.40	10.13	Pu 239	15.74	15.42
Cm 240	6.28	6.27	Bk 249	8.78	8.67
242	6.86	7.27	Cf 249	9.18	8.65
244	7.15	7.09	E 253	5.48	4.38
246	7.48	7.88	Fm 255	1.30	2.79
			Odd-odd nuclei		
			E 254	5.18	5.17

[a] The experimental values are from a summary by A. Ghiorso, kindly lent to me by Professor S. G. Thompson.

The importance of shell structure in the fission process is suggested by the fact that, according to the present considerations, the oscillations of the masses (associated with individual particle structure) in the range $\delta M=1-3$ mMU shorten the lifetimes by factors of 10^5 to 10^{15}. On the other hand the irregularities in the original plot of τ_{exp} against Z^2/A are seen to be largely due to irregularities in the ground-state masses, associated with *shell structure in the ground-state configuration*. The smoothness of the points $\tau_{\text{exp}}+k\delta M$ suggests that, after correcting for shell structure in the ground-state configuration, the description of the fission process in terms of a model in which single-particle features are treated in an average way may be useful. Qualitative reasons for the greater validity of such an averaged description for the more strongly deformed nuclear shapes occurring in fission may be found in the disappearance for such shapes of degeneracies in the energy spectrum associated with the proximity to a spherically symmetric configuration.

It is a pleasure to acknowledge discussions with Professor S. G. Thompson and Dr. A. C. Pappas and stimulating contacts with Dr. Aage Bohr and Dr. B. R. Mottelson and members of the C.E.R.N. Theoretical Study Group in Copenhagen.

[1] See for example J. R. Huizenga, Phys. Rev. **94**, 158 (1954).
[2] The existence of correlations between nuclear masses, fission thresholds, and half-lives has been considered by Professor D. Frisch, to whom I am greatly indebted for stimulating discussions.
[3] A. E. S. Green, Phys. Rev. **95**, 1006 (1954).
[4] Glass, Thompson, and Seaborg, J. Inorg. Nuc. Chem. **1**, 3 (1955).

Potential Energy of Deformation

We use the macroscopic-microscopic method introduced by Swiatecki and Strutinsky:

$$E_{\mathrm{pot}}(\mathrm{shape}) = E_{\mathrm{macr}}(\mathrm{shape}) + E_{\mathrm{micr}}(\mathrm{shape}) \quad (1)$$

The macroscopic term is calculated in a liquid-drop type model (for a specific deformed shape).

The microscopic correction is determined in the following steps

1. A shape is prescribed
2. A single-particle potential with this shape is generated. A spin-orbit term is included.
3. The Schrödinger equation is solved for this deformed potential and single-particle levels and wave-functions are obtained
4. The shell correction is calculated by use of Strutinsky's method.
5. The pairing correction is calculated in the BCS or Lipkin-Nogami method.

Shape Parameterizations

For small distortions we use multipole expansions, for example the β parameterization:

$$r(\theta,\phi) = R_0(1 + \sum_{l=1}^{\infty} \sum_{m=-l}^{l} \beta_{lm} Y_l^m)$$

For large deformations near the outer saddle in the actinide region or beyond we use the three-quadratic-surface parameterization:

$$\rho(z)^2 = \begin{cases} {a_1}^2 - \dfrac{{a_1}^2}{{c_1}^2}(z-l_1)^2 \quad , \quad l_1 - c_1 \leq z \leq z_1 \\ {a_2}^2 - \dfrac{{a_2}^2}{{c_2}^2}(z-l_2)^2 \quad , \quad z_2 \leq z \leq l_2 + c_2 \\ {a_3}^2 - \dfrac{{a_3}^2}{{c_3}^2}(z-l_3)^2 \quad , \quad z_1 \leq z \leq z_2 \end{cases}$$

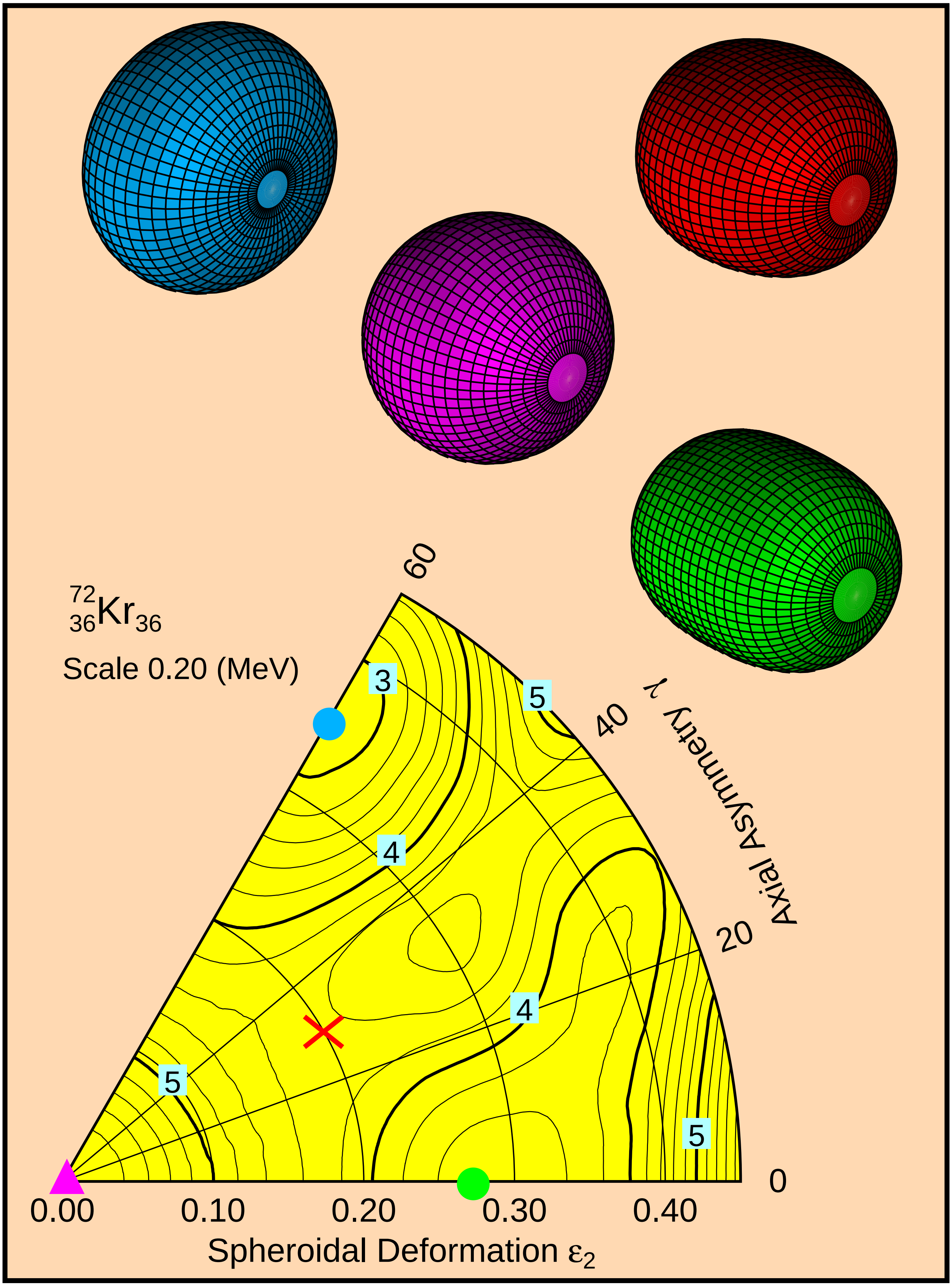

$^{72}_{36}Kr_{36}$
Scale 0.20 (MeV)
60
40
20
0
Axial Asymmetry γ
3
4
5
4
5
5
0.00
0.10
0.20
0.30
0.40
Spheroidal Deformation ε_2

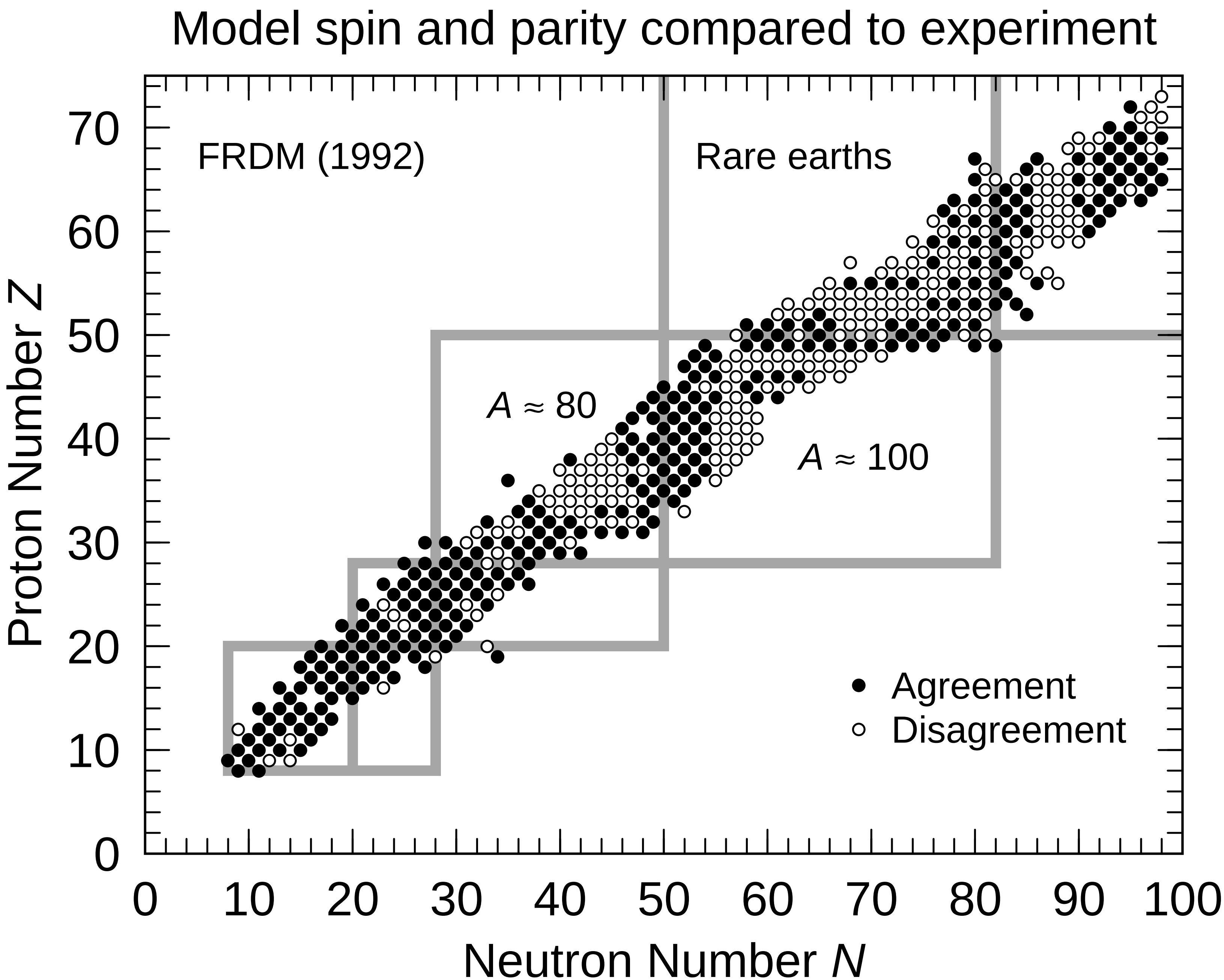

Model spin and parity compared to experiment
FRDM (1992)
Rare earths
A ≈ 80
A ≈ 100
Agreement
Disagreement
Proton Number Z
Neutron Number N
0
10
20
30
40
50
60
70
80
90
100

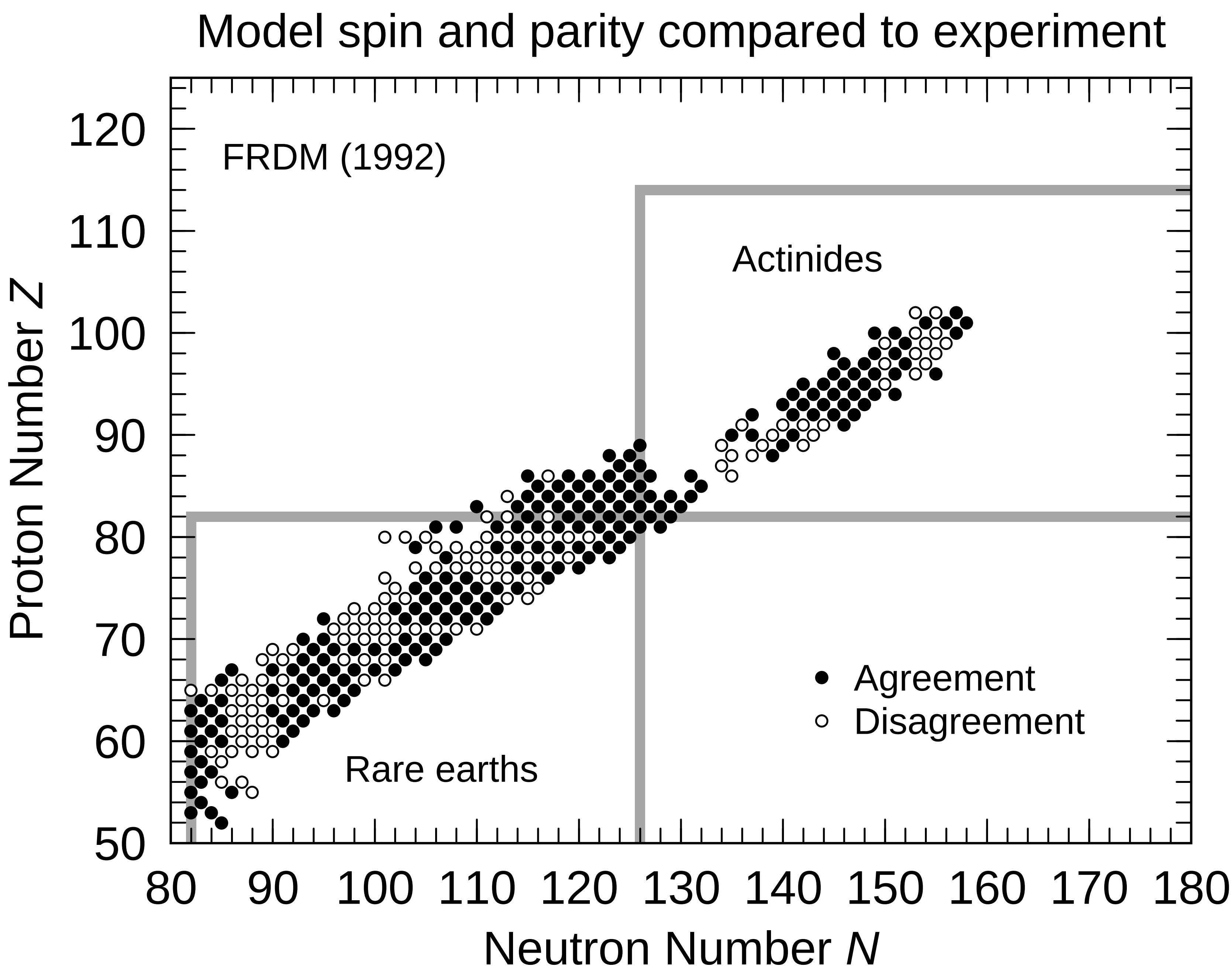

Model spin and parity compared to experiment
FRDM (1992)
Actinides
Rare earths
Agreement
Disagreement
Proton Number Z
Neutron Number N
120
110
100
90
80
70
60
50
80
90
100
110
120
130
140
150
160
170
180

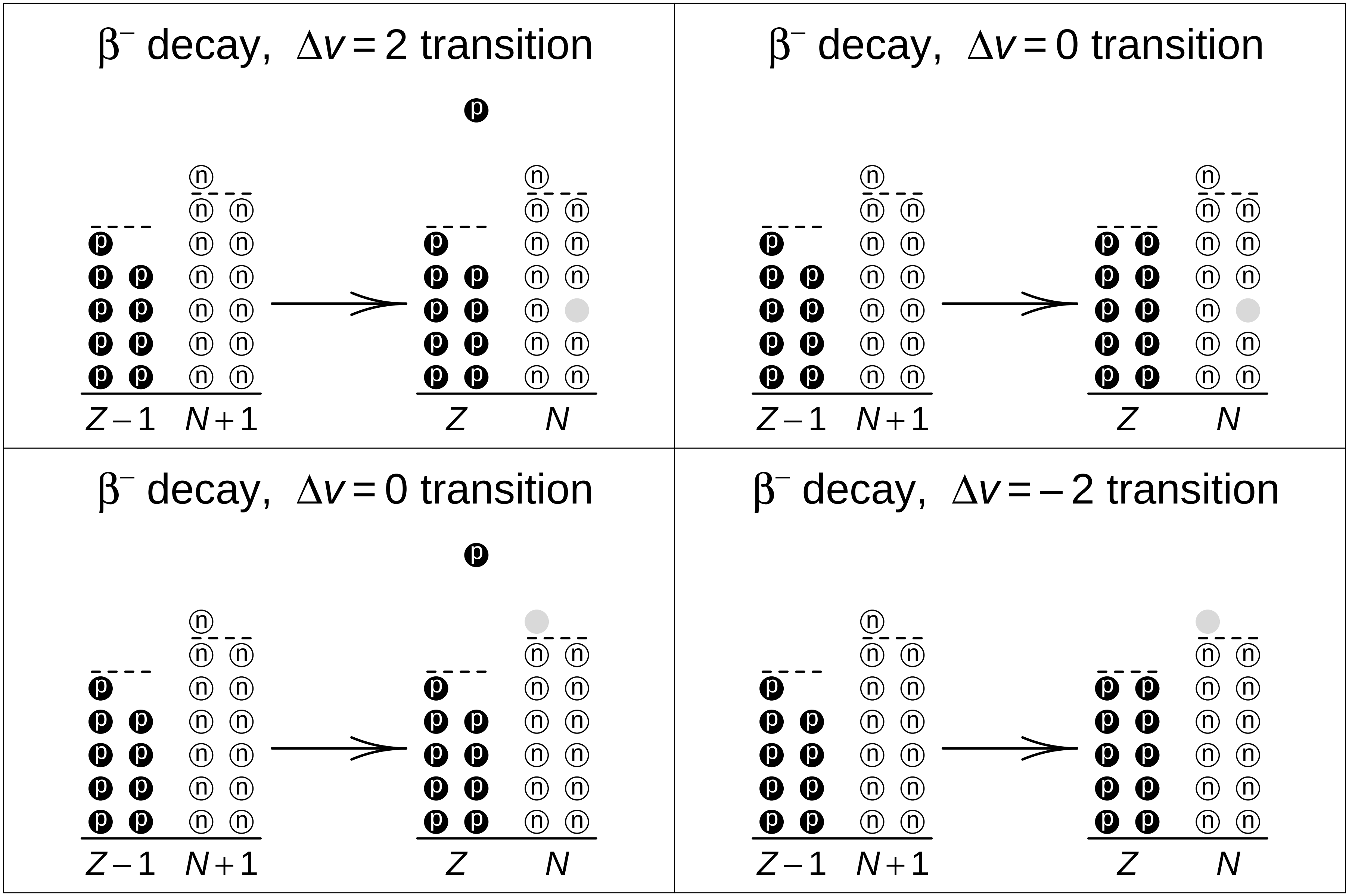

β⁻ decay, Δv = 2 transition
β⁻ decay, Δv = 0 transition
β⁻ decay, Δv = 0 transition
β⁻ decay, Δv = −2 transition
p
n
Z − 1
N + 1
Z
N

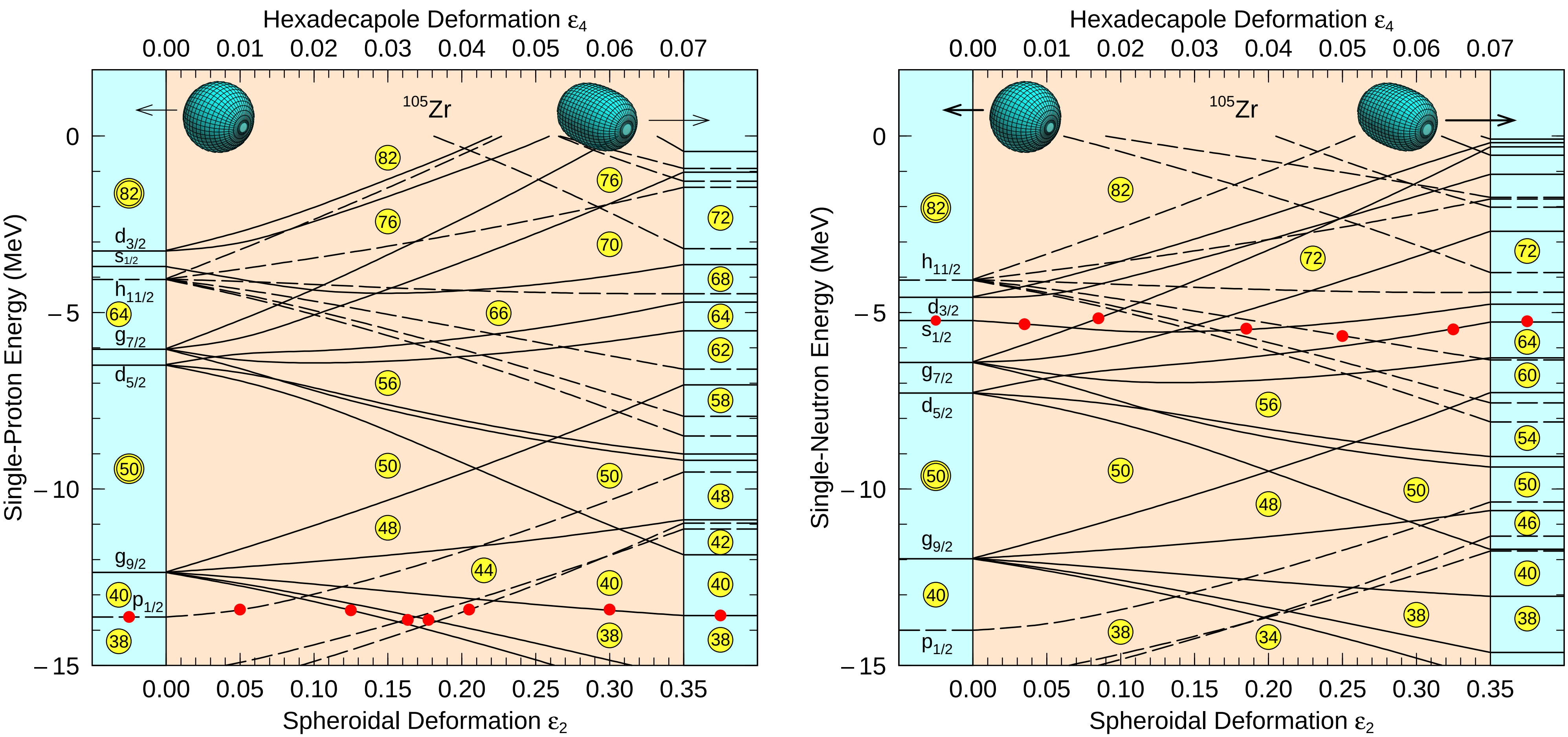

Hexadecapole Deformation ε4
0.00 0.01 0.02 0.03 0.04 0.05 0.06 0.07
105Zr
Single-Proton Energy (MeV)
0
−5
−10
−15
d3/2
s1/2
h11/2
g7/2
d5/2
g9/2
p1/2
82 64 50 40 38
82 76 56 50 48
66 44
76 70 50 40 38
72 68 64 62 58 48 42 40 38
0.00 0.05 0.10 0.15 0.20 0.25 0.30 0.35
Spheroidal Deformation ε2
Hexadecapole Deformation ε4
0.00 0.01 0.02 0.03 0.04 0.05 0.06 0.07
105Zr
Single-Neutron Energy (MeV)
0
−5
−10
−15
h11/2
d3/2
s1/2
g7/2
d5/2
g9/2
p1/2
82 50 40
82 50 38
72 56 48 34
50 38
72 64 60 54 50 46 40 38
0.00 0.05 0.10 0.15 0.20 0.25 0.30 0.35
Spheroidal Deformation ε2

Nuclear Physics A417 (1984) 419–446

CALCULATION OF GAMOW–TELLER β-STRENGTH FUNCTIONS IN THE RUBIDIUM REGION IN THE RPA APPROXIMATION WITH NILSSON-MODEL WAVE FUNCTIONS

JOACHIM KRUMLINDE and PETER MÖLLER

Departments of Physics and Mathematical Physics, Lund University, Box 725, S22007 Lund, Sweden

Received 14 March 1983
(Revised 3 August 1983)

Abstract: We calculate allowed Gamow–Teller and, in a few cases, Fermi β-strength functions in a model that is applicable to studies of nuclei throughout the periodic system. For our first study we have selected a sequence of rubidium isotopes, namely $^{89}_{37}$Rb–$^{99}_{37}$Rb. We develop a model that uses calculated Nilsson-model wave functions, spherical or deformed, as the case may be, as the starting point for determining the wave functions of the mother and daughter nuclei in the β-decay. Pairing is treated in the BCS approximation. To account for the retardation of low-energy GT decay rates we add, as is customarily done, a simple residual interaction specific to GT decay, namely $V_{GT} = :\beta^{1-}\beta^{1+}:$, to the hamiltonian. This residual interaction is treated in the RPA approximation. The strength of the interaction is adjusted to get agreement between the calculated and experimental energy of the giant Gamow–Teller resonance for ^{208}Pb and ^{144}Sm. Since the present model is based on calculated wave functions and single-particle levels, studies of nuclei far from stability, where little experimental information is available, are more straightforward relative to calculations where "experimental" levels are used. The model can treat deformed nuclei employing wave functions calculated to desired accuracy, within the framework of the model, for the deformed single-particle well. The calculations show that use of single-particle parameters appropriate to the region studied and taking deformation into account is important. We find good agreement between calculated and experimental spectra over the region studied, provided an appropriate choice of single-particle parameters and deformation is made.

1. Introduction

A theoretical understanding of β-strength functions is important for the interpretation of the large amount of experimental data that is now being collected on, for instance, the giant Gamow–Teller resonance [1–2]) and on β-decay spectra of nuclei far from stability [3]). More references on these subjects are found in the conference report [4]) of the 4th International Conference on Nuclei far from Stability and references quoted therein. The β-strength function must also be known for theoretical studies of phenomena where the β-strength function cannot be easily measured. Examples of such processes are the decay from the r-process line to the line of β-stability [5–7]), β-delayed particle emission [7]) and the production of transuranium elements by neutron capture and subsequent decay by β-emission, fission and neutron emission [8,9]).

A variety of models have been used to calculate β-strength functions. The gross theory of β-decay [10]) describes, because of its statistical character, only the average

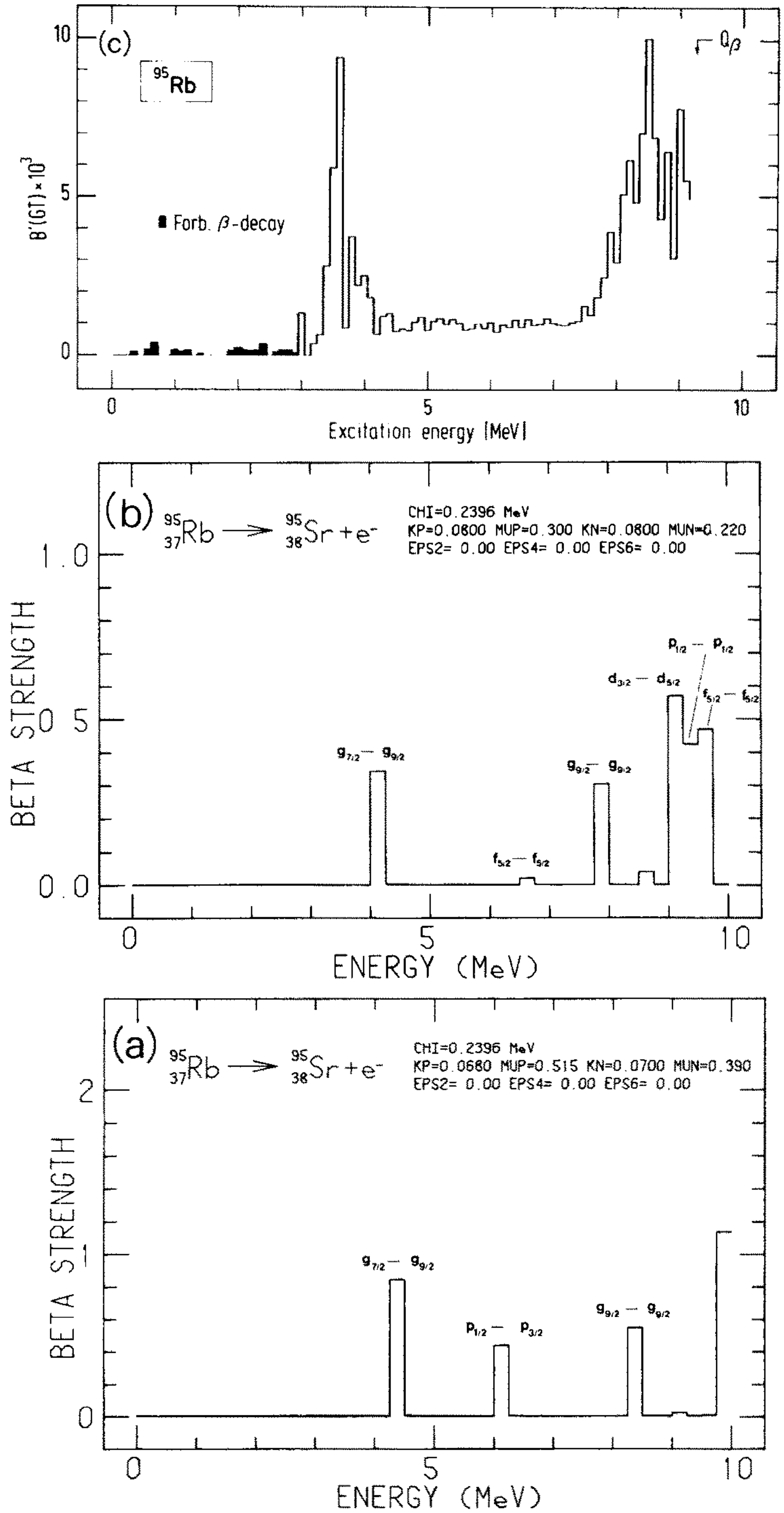

Fig. 8. Calculated β^- GT strength function for ^{95}Rb with (a) the $A=100$ set of κ and μ, and (b) the $N=60$ set of κ and μ, in units of $4f^2$ MeV^{-1}. The peaks are labeled with the quantum numbers of the neutron (first) and proton (last) orbital involved in the transition. (c) Experimental results from ref. [3]).

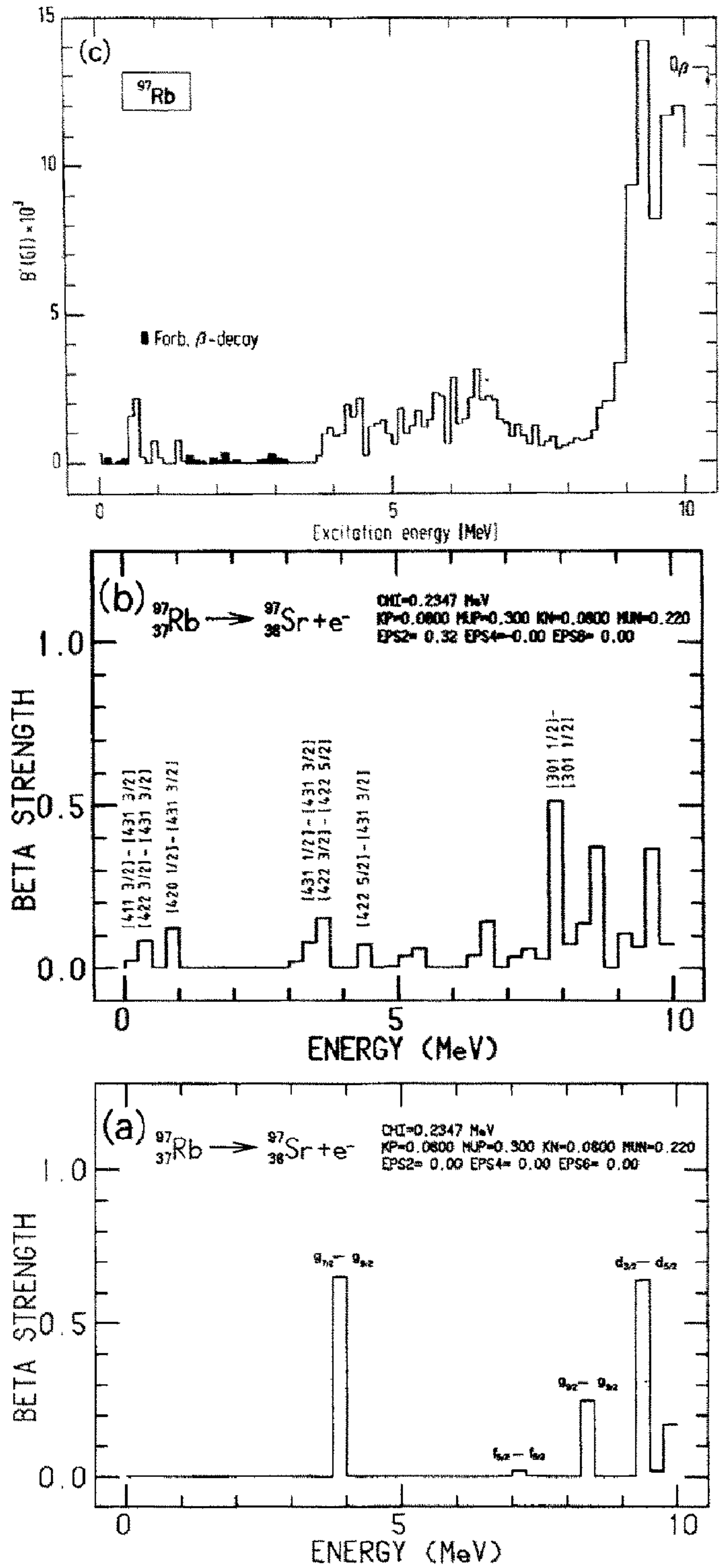

Fig. 9. Calculated β^- GT strength function for ^{97}Rb treated as (a) a spherical nucleus, and (b) a deformed nucleus, in units of $4f^2$ MeV^{-1}. The peaks in (b) are labeled with the asymptotic quantum numbers of the neutron (first) and proton (last) orbital involved in the transition. (c) Experimental results from ref. [3]).

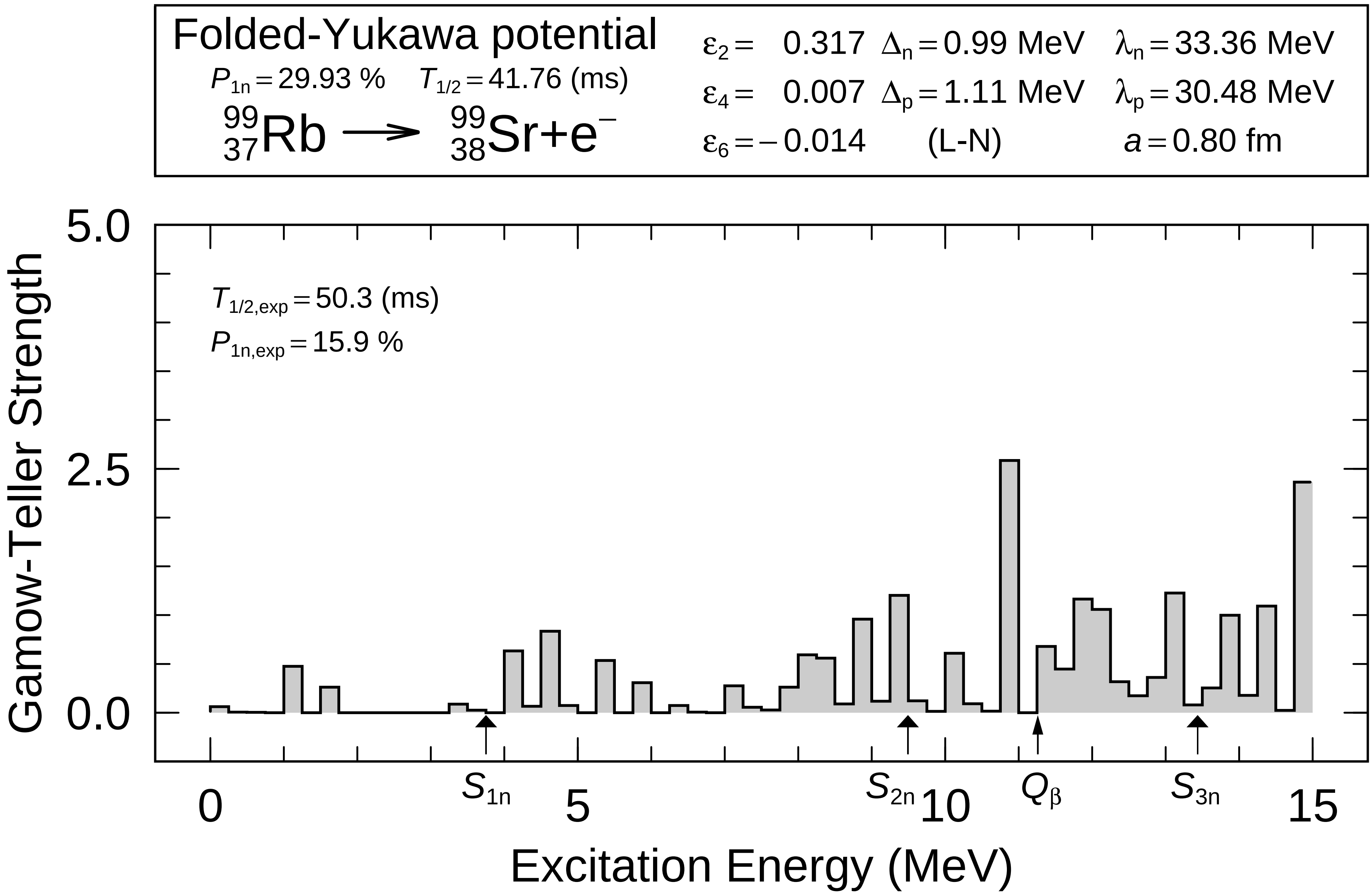

Folded-Yukawa potential
P1n = 29.93 %
T1/2 = 41.76 (ms)
99 37Rb ⟶ 99 38Sr+e−
ε2 = 0.317
Δn = 0.99 MeV
λn = 33.36 MeV
ε4 = 0.007
Δp = 1.11 MeV
λp = 30.48 MeV
ε6 = −0.014
(L-N)
a = 0.80 fm
T1/2,exp = 50.3 (ms)
P1n,exp = 15.9 %
Gamow-Teller Strength
5.0
2.5
0.0
S1n
S2n
Qβ
S3n
0
5
10
15
Excitation Energy (MeV)

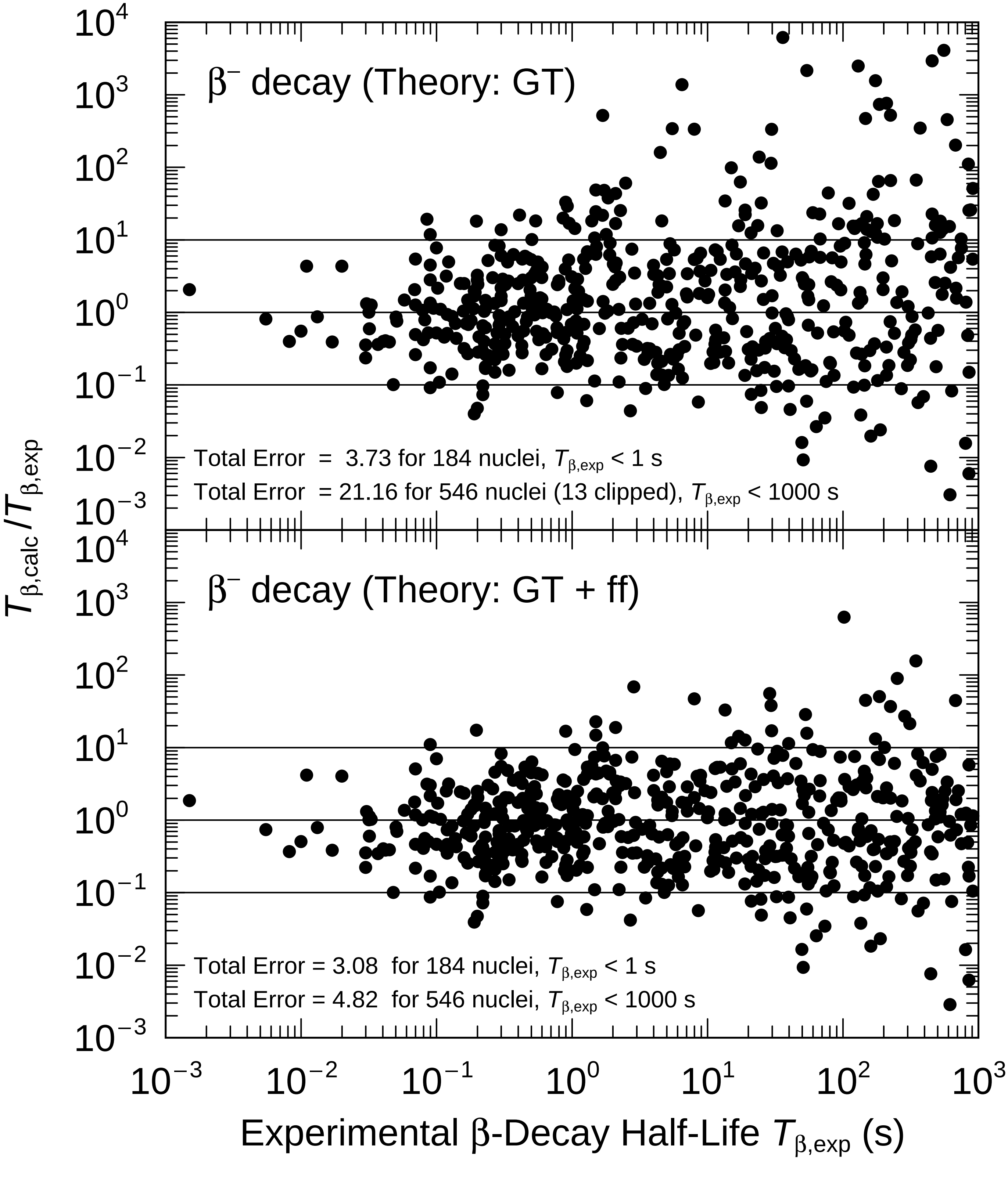

β⁻ decay (Theory: GT)
Total Error = 3.73 for 184 nuclei, $T_{\beta,\mathrm{exp}}$ < 1 s
Total Error = 21.16 for 546 nuclei (13 clipped), $T_{\beta,\mathrm{exp}}$ < 1000 s
β⁻ decay (Theory: GT + ff)
Total Error = 3.08 for 184 nuclei, $T_{\beta,\mathrm{exp}}$ < 1 s
Total Error = 4.82 for 546 nuclei, $T_{\beta,\mathrm{exp}}$ < 1000 s
$T_{\beta,\mathrm{calc}}/T_{\beta,\mathrm{exp}}$
Experimental β-Decay Half-Life $T_{\beta,\mathrm{exp}}$ (s)

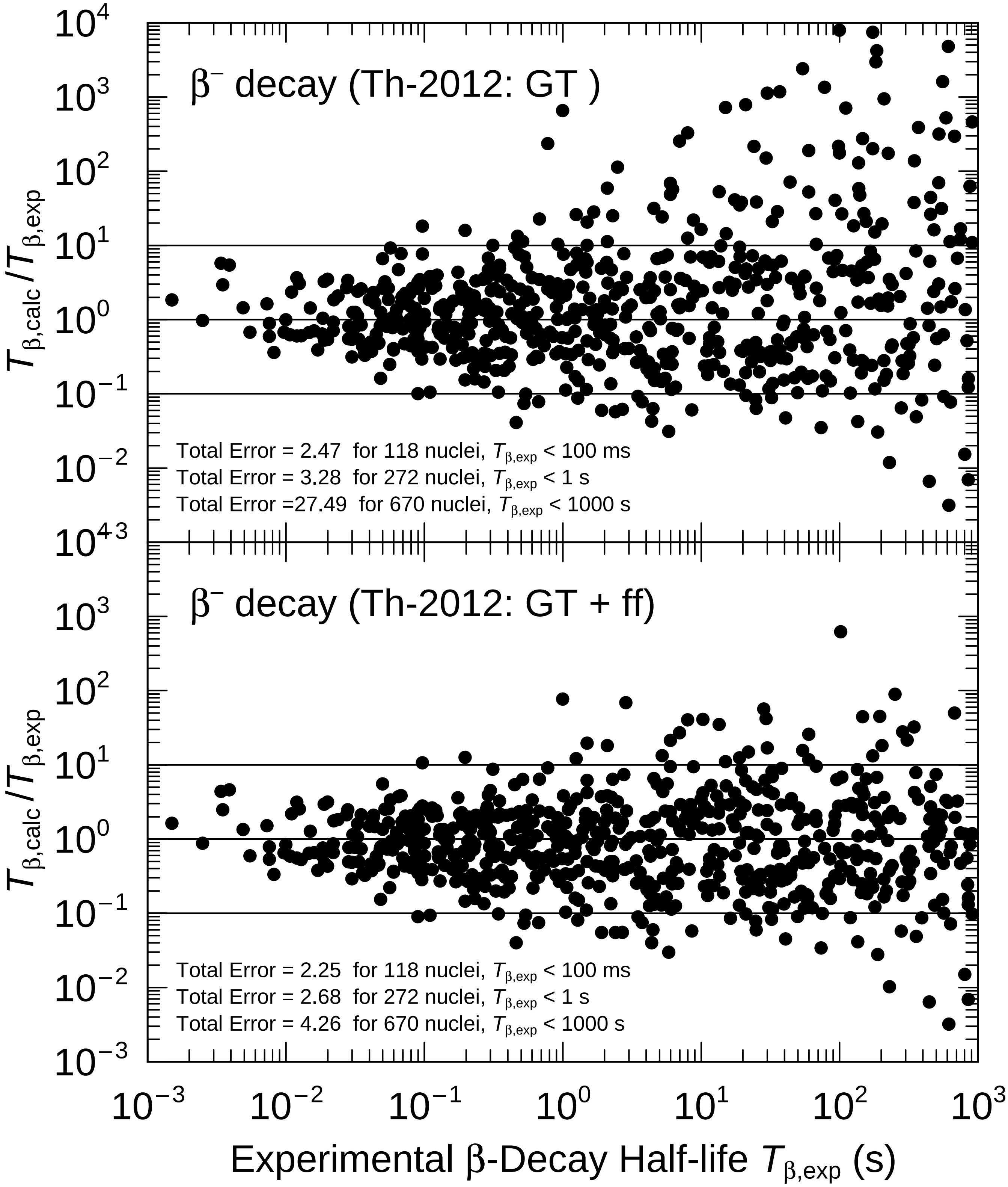

β⁻ decay (Th-2012: GT)
Total Error = 2.47 for 118 nuclei, $T_{\beta,\mathrm{exp}}$ < 100 ms
Total Error = 3.28 for 272 nuclei, $T_{\beta,\mathrm{exp}}$ < 1 s
Total Error =27.49 for 670 nuclei, $T_{\beta,\mathrm{exp}}$ < 1000 s
β⁻ decay (Th-2012: GT + ff)
Total Error = 2.25 for 118 nuclei, $T_{\beta,\mathrm{exp}}$ < 100 ms
Total Error = 2.68 for 272 nuclei, $T_{\beta,\mathrm{exp}}$ < 1 s
Total Error = 4.26 for 670 nuclei, $T_{\beta,\mathrm{exp}}$ < 1000 s
$T_{\beta,\mathrm{calc}}/T_{\beta,\mathrm{exp}}$
Experimental β-Decay Half-life $T_{\beta,\mathrm{exp}}$ (s)

Table 1: Analysis of the discrepancy between calculated (with our 1997–2003 models) and measured β^--decay half-lives. The experimental data file is Nubase12. The number of 0.1s half-lives increased from 42 to 118.

Model	n	M_{r_1}	$M_{r_1}^{10}$	σ_{r_1}	$\sigma_{r_1}^{10}$	Σ_{r_1}	$\Sigma_{r_1}^{10}$	$T_{\beta,\mathrm{exp}}^{\mathrm{max}}$ (s)
GT	670	0.38	2.39	1.22	16.47	1.27	18.79	1000.00
GT + FF	670	0.02	1.04	0.64	4.36	0.64	4.36	1000.00
GT	552	0.28	1.89	0.98	9.45	1.01	10.32	100.00
GT + FF	552	0.02	1.06	0.57	3.73	0.57	3.73	100.00
GT	414	0.20	1.59	0.71	5.16	0.74	5.50	10.00
GT + FF	414	0.04	1.10	0.51	3.21	0.51	3.22	10.00
GT	272	0.15	1.42	0.54	3.49	0.56	3.66	1.00
GT + FF	272	0.04	1.09	0.43	2.70	0.43	2.71	1.00
GT	229	0.11	1.29	0.47	2.97	0.49	3.06	0.50
GT + FF	229	0.02	1.06	0.41	2.59	0.41	2.60	0.50
GT	159	0.08	1.21	0.45	2.79	0.45	2.84	0.20
GT + FF	159	0.02	1.04	0.40	2.53	0.40	2.54	0.20
GT	118	0.07	1.18	0.43	2.72	0.44	2.76	0.10
GT + FF	118	0.01	1.02	0.39	2.44	0.39	2.44	0.10
GT	67	0.04	1.10	0.37	2.36	0.38	2.37	0.05
GT + FF	67	0.00	1.01	0.36	2.28	0.36	2.28	0.05
GT	29	0.11	1.29	0.34	2.21	0.36	2.30	0.02
GT + FF	29	0.07	1.19	0.34	2.17	0.35	2.21	0.02

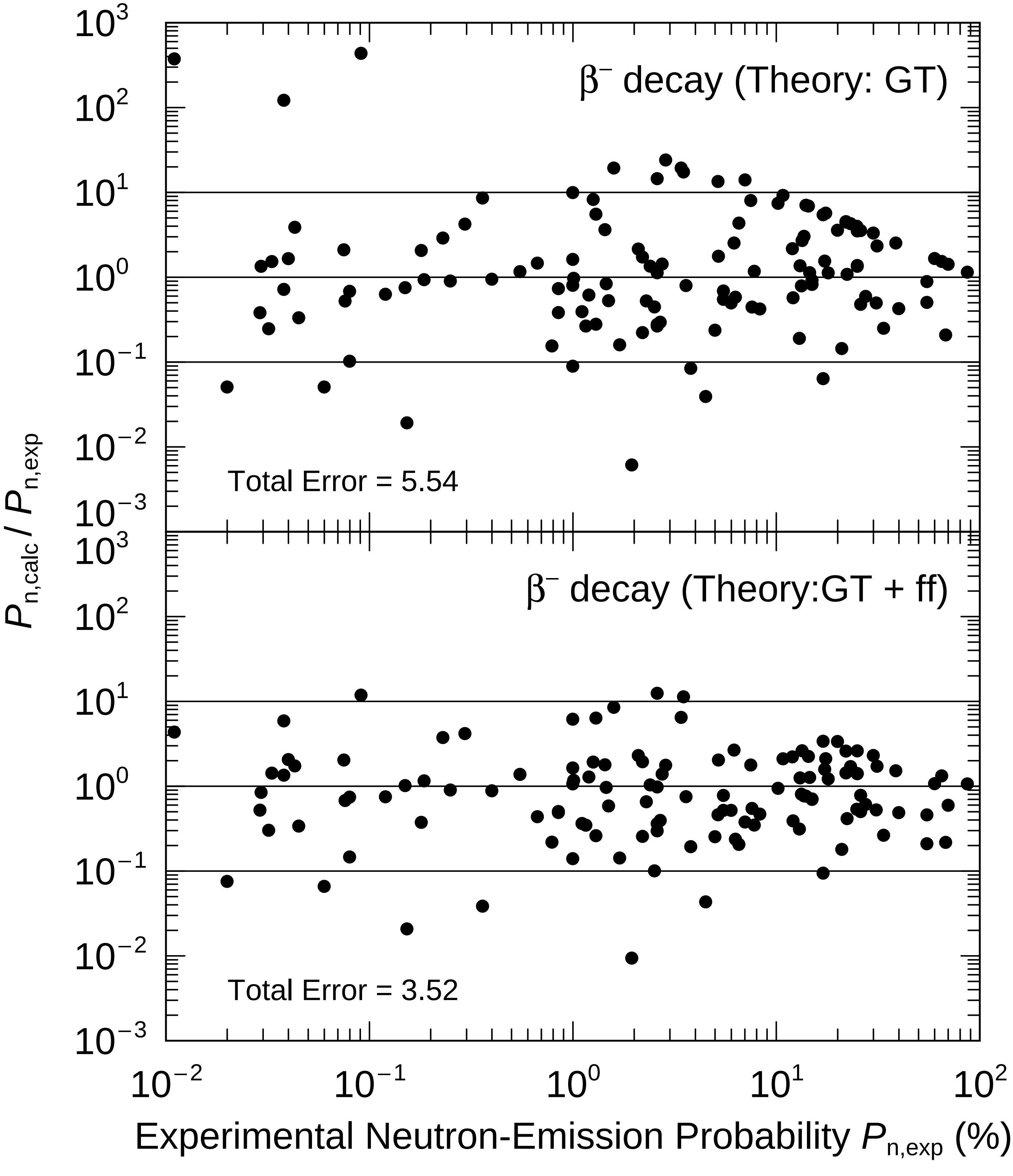

β⁻ decay (Theory: GT)
Total Error = 5.54
β⁻ decay (Theory:GT + ff)
Total Error = 3.52
$P_{n,calc} / P_{n,exp}$
Experimental Neutron-Emission Probability $P_{n,exp}$ (%)
10^{-3}
10^{-2}
10^{-1}
10^{0}
10^{1}
10^{2}
10^{3}

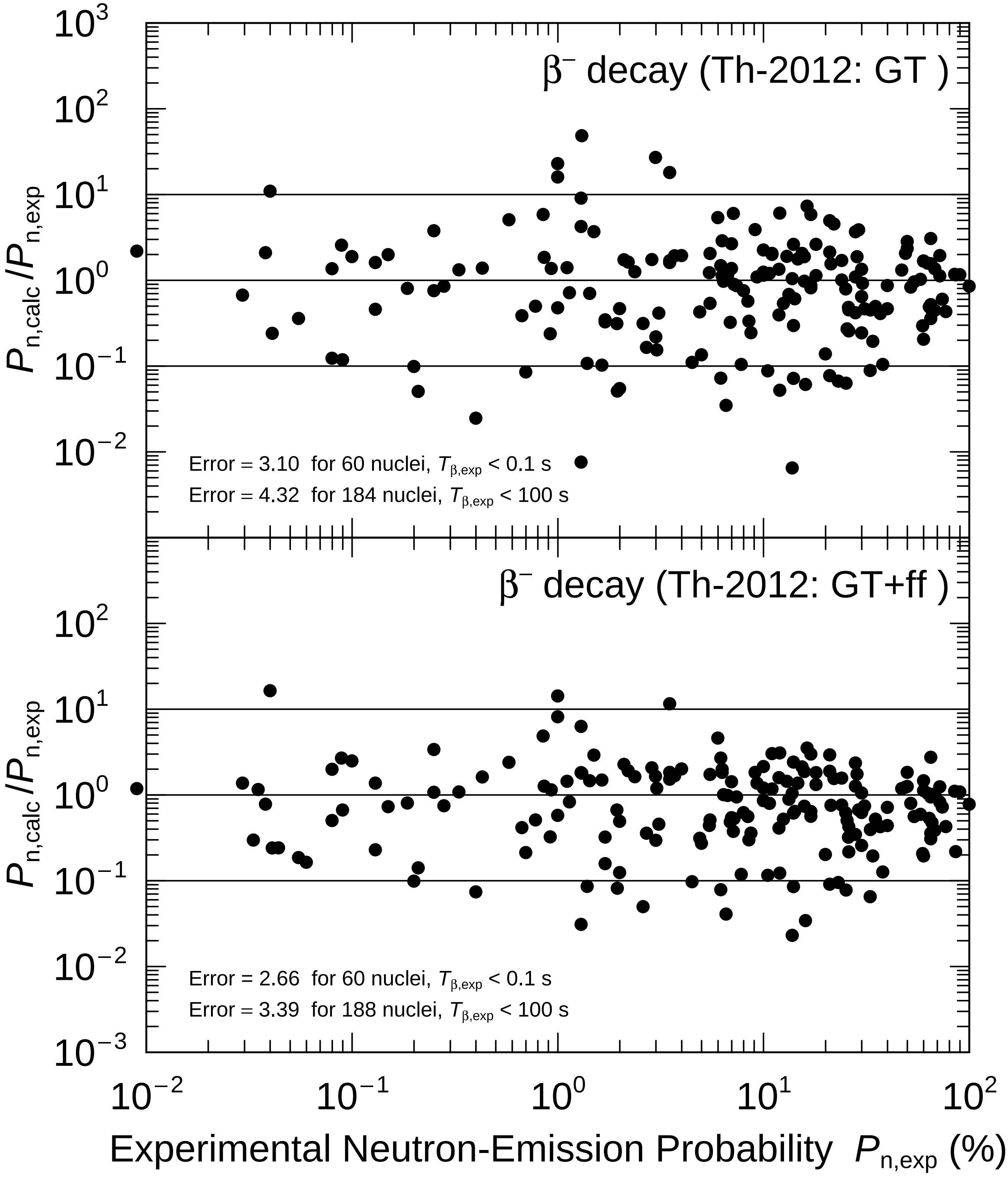

β⁻ decay (Th-2012: GT)
Error = 3.10 for 60 nuclei, $T_{\beta,exp}$ < 0.1 s
Error = 4.32 for 184 nuclei, $T_{\beta,exp}$ < 100 s
β⁻ decay (Th-2012: GT+ff)
Error = 2.66 for 60 nuclei, $T_{\beta,exp}$ < 0.1 s
Error = 3.39 for 188 nuclei, $T_{\beta,exp}$ < 100 s
$P_{n,calc}/P_{n,exp}$
Experimental Neutron-Emission Probability $P_{n,exp}$ (%)

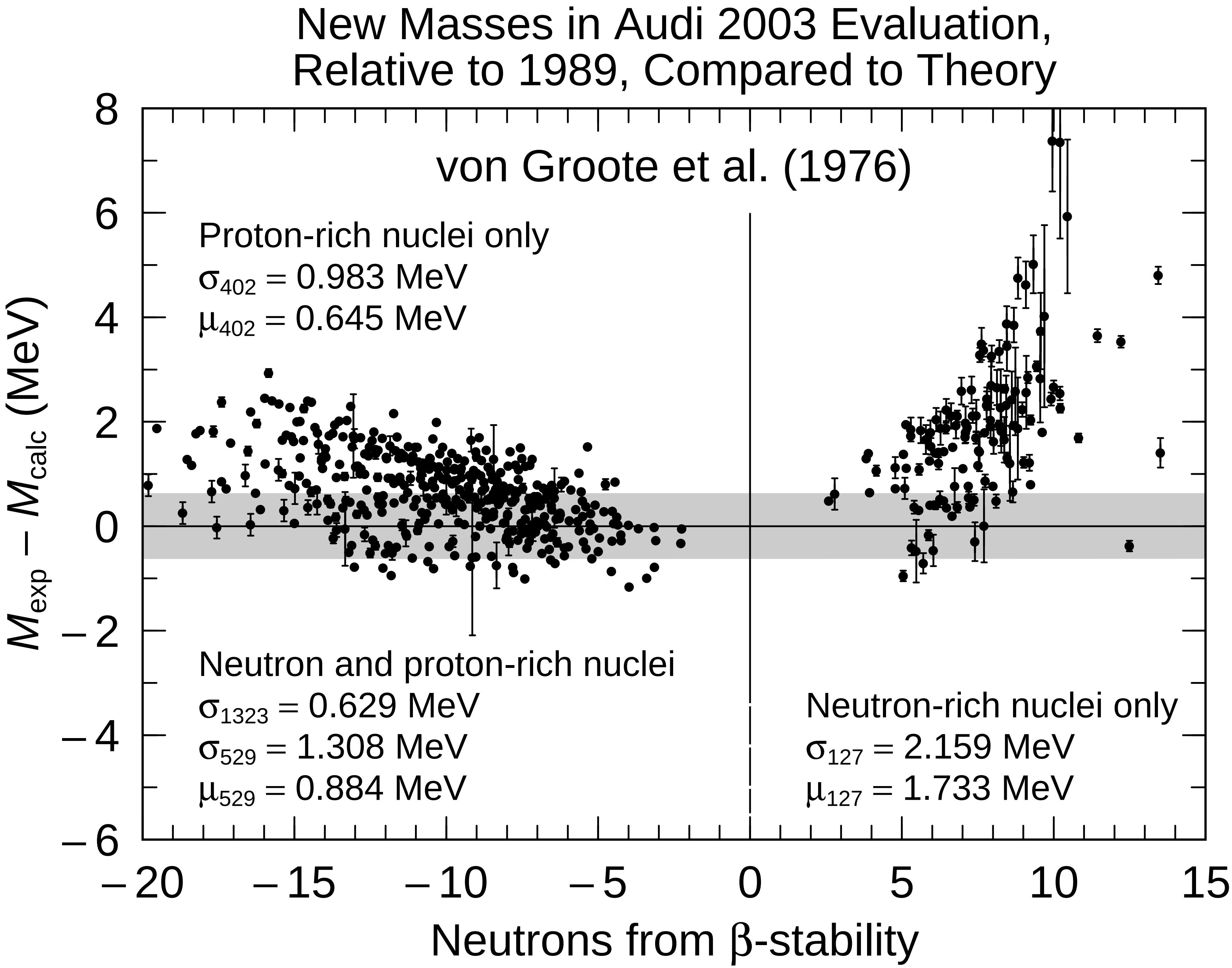
New Masses in Audi 2003 Evaluation,
Relative to 1989, Compared to Theory
von Groote et al. (1976)
Proton-rich nuclei only
$\sigma_{402} = 0.983$ MeV
$\mu_{402} = 0.645$ MeV
Neutron and proton-rich nuclei
$\sigma_{1323} = 0.629$ MeV
$\sigma_{529} = 1.308$ MeV
$\mu_{529} = 0.884$ MeV
Neutron-rich nuclei only
$\sigma_{127} = 2.159$ MeV
$\mu_{127} = 1.733$ MeV
$M_{exp} - M_{calc}$ (MeV)
Neutrons from β-stability
8
6
4
2
0
−2
−4
−6
−20
−15
−10
−5
0
5
10
15

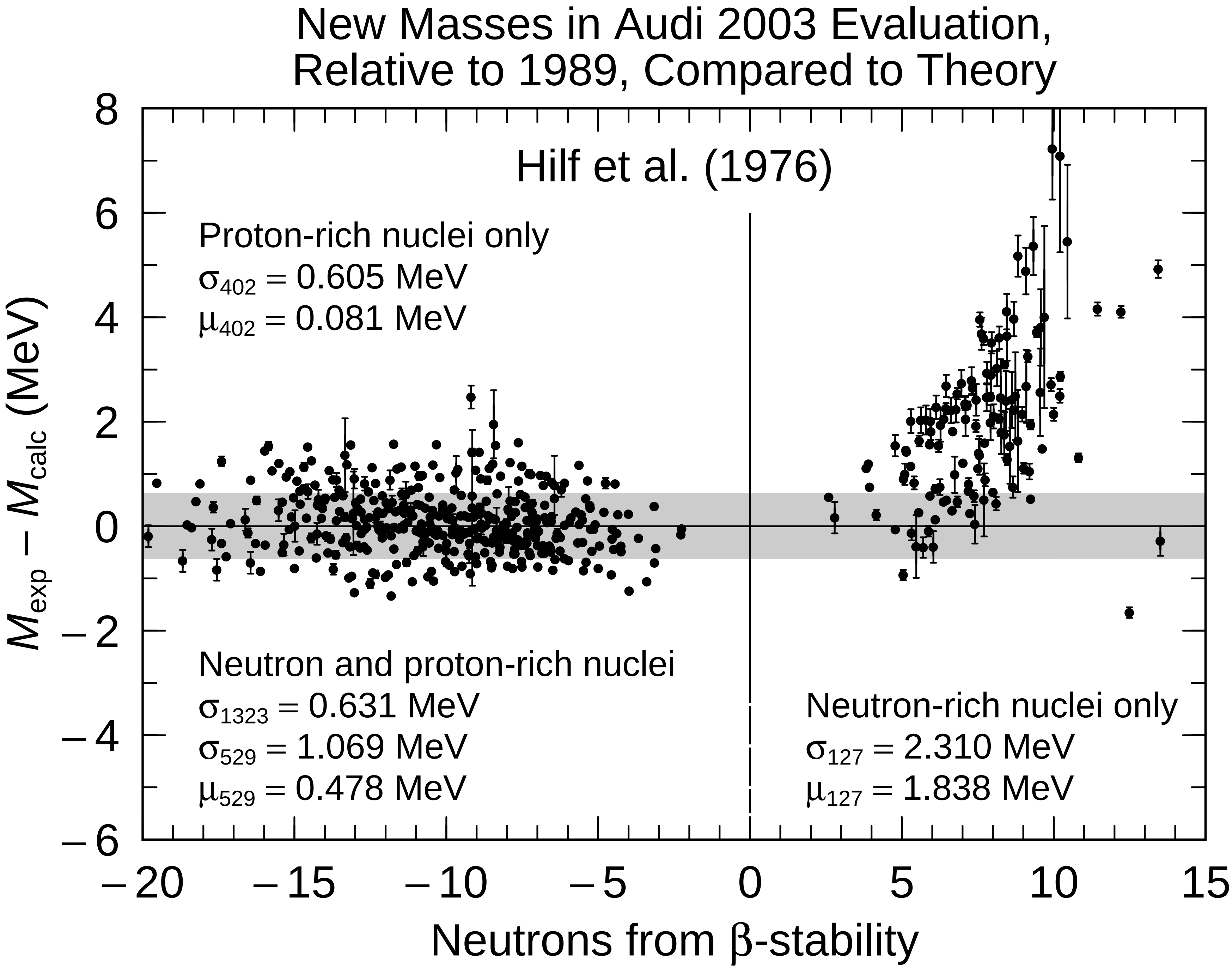
New Masses in Audi 2003 Evaluation,
Relative to 1989, Compared to Theory
Hilf et al. (1976)
Proton-rich nuclei only
σ402 = 0.605 MeV
μ402 = 0.081 MeV
Neutron and proton-rich nuclei
σ1323 = 0.631 MeV
σ529 = 1.069 MeV
μ529 = 0.478 MeV
Neutron-rich nuclei only
σ127 = 2.310 MeV
μ127 = 1.838 MeV
Mexp − Mcalc (MeV)
Neutrons from β-stability
8
6
4
2
0
−2
−4
−6
−20
−15
−10
−5
0
5
10
15

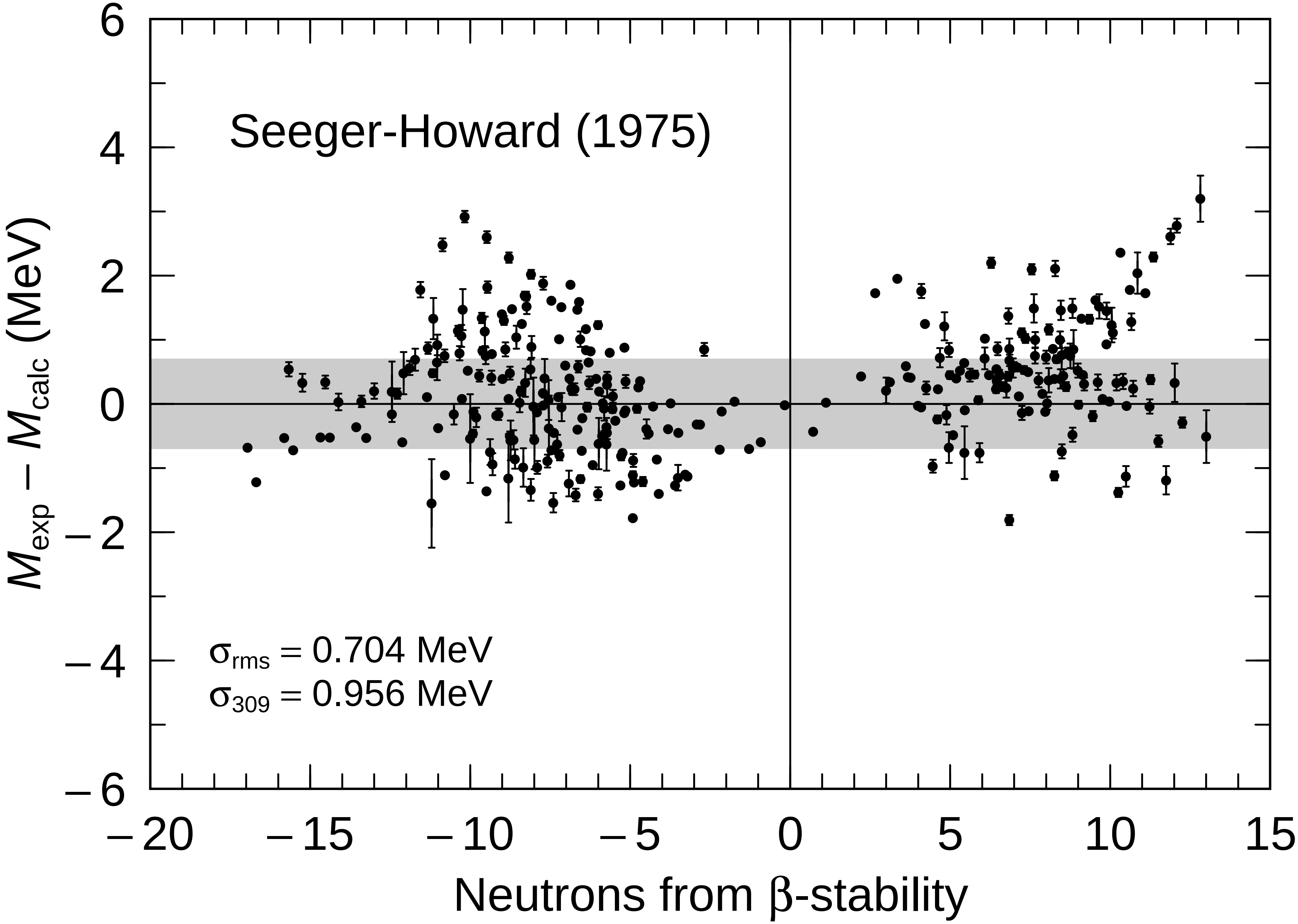

Seeger-Howard (1975)
$\sigma_{rms} = 0.704$ MeV
$\sigma_{309} = 0.956$ MeV
$M_{exp} - M_{calc}$ (MeV)
Neutrons from β-stability
6
4
2
0
−2
−4
−6
−20
−15
−10
−5
0
5
10
15

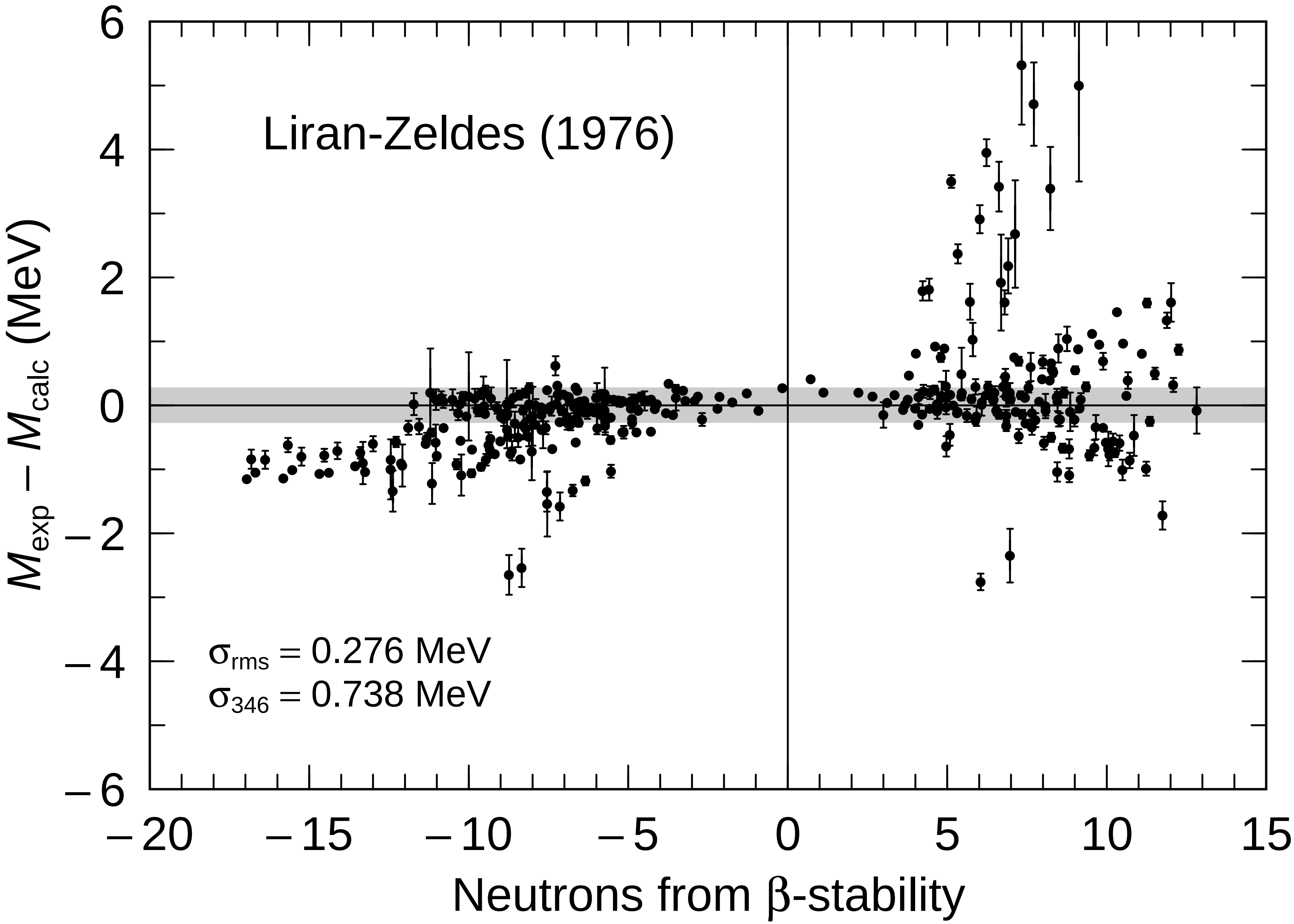
Liran-Zeldes (1976)
σ_{rms} = 0.276 MeV
σ_{346} = 0.738 MeV
$M_{exp} - M_{calc}$ (MeV)
Neutrons from β-stability
6
4
2
0
−2
−4
−6
−20
−15
−10
−5
0
5
10
15

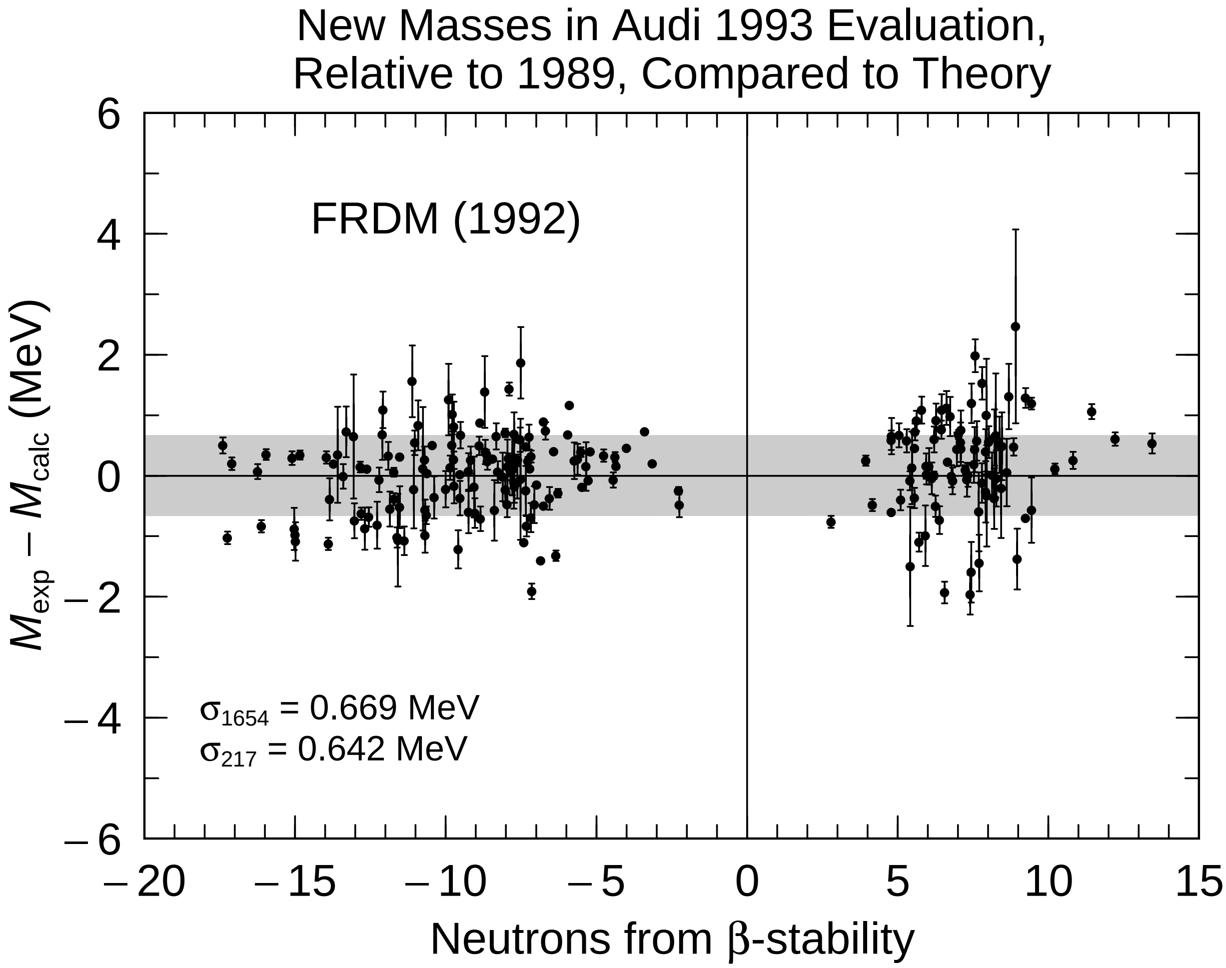
New Masses in Audi 1993 Evaluation,
Relative to 1989, Compared to Theory
FRDM (1992)
σ_{1654} = 0.669 MeV
σ_{217} = 0.642 MeV
$M_{exp} - M_{calc}$ (MeV)
Neutrons from β-stability
6
4
2
0
−2
−4
−6
−20
−15
−10
−5
0
5
10
15

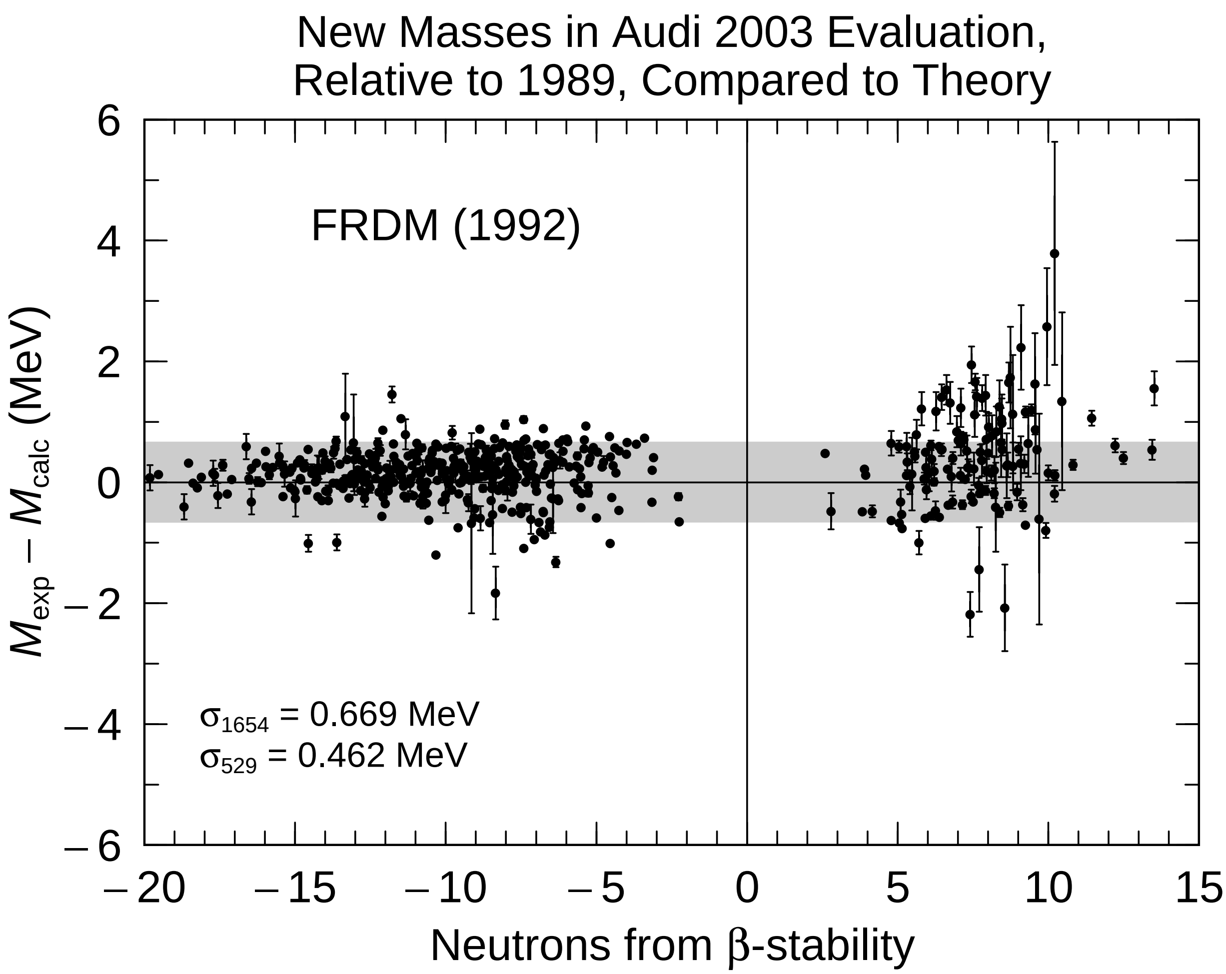
New Masses in Audi 2003 Evaluation,
Relative to 1989, Compared to Theory
FRDM (1992)
σ_{1654} = 0.669 MeV
σ_{529} = 0.462 MeV
$M_{exp} - M_{calc}$ (MeV)
Neutrons from β-stability
6
4
2
0
−2
−4
−6
−20
−15
−10
−5
0
5
10
15

Successive FRDM enhancements

Optimization (2006)

Better search for optimum FRDM parameters.

Accuracy improvement: 0.01 MeV

New mass data base (AME2003) (2006)

Better agreement than with AME1989.

Accuracy improvement: 0.04 MeV

Full 4D energy minimization (2006–2008)

Full 4D minimization($\epsilon_2, \epsilon_3, \epsilon_4, \epsilon_6$) step=0.01.

Accuracy improvement: 0.02 MeV

Axial asymmetry (2002–2006)

Also yields correct SHE gs assignments.

Accuracy improvement: 0.01 MeV

L **variation** (2009–2011)

Accuracy improvement: 0.02 MeV

Improved gs correlation energies (2012)

Accuracy improvement: 0.01 MeV

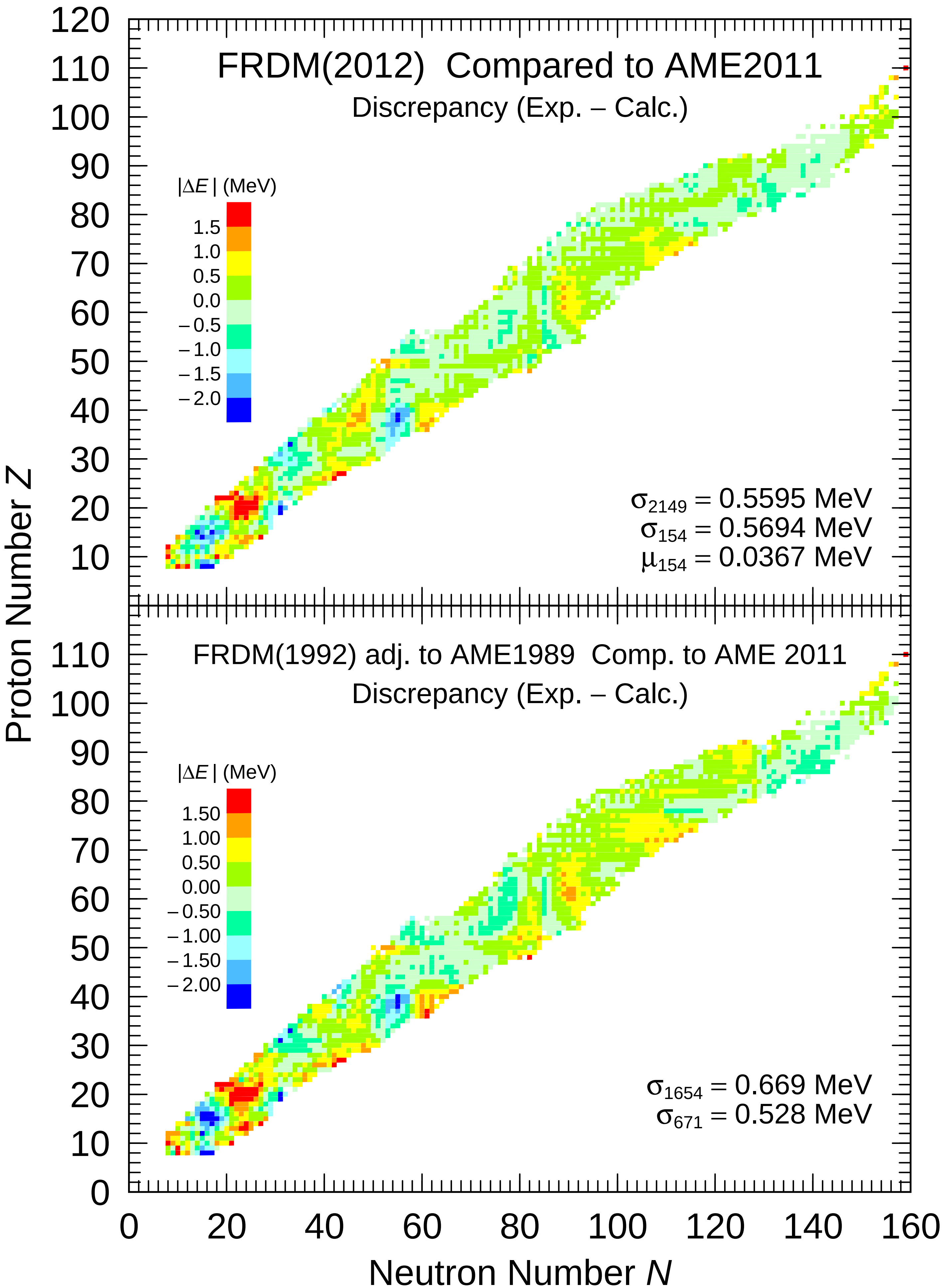

FRDM(2012) Compared to AME2011
Discrepancy (Exp. – Calc.)
|ΔE| (MeV)
1.5
1.0
0.5
0.0
−0.5
−1.0
−1.5
−2.0
σ2149 = 0.5595 MeV
σ154 = 0.5694 MeV
μ154 = 0.0367 MeV
FRDM(1992) adj. to AME1989 Comp. to AME 2011
Discrepancy (Exp. – Calc.)
|ΔE| (MeV)
1.50
1.00
0.50
0.00
−0.50
−1.00
−1.50
−2.00
σ1654 = 0.669 MeV
σ671 = 0.528 MeV
Proton Number Z
Neutron Number N

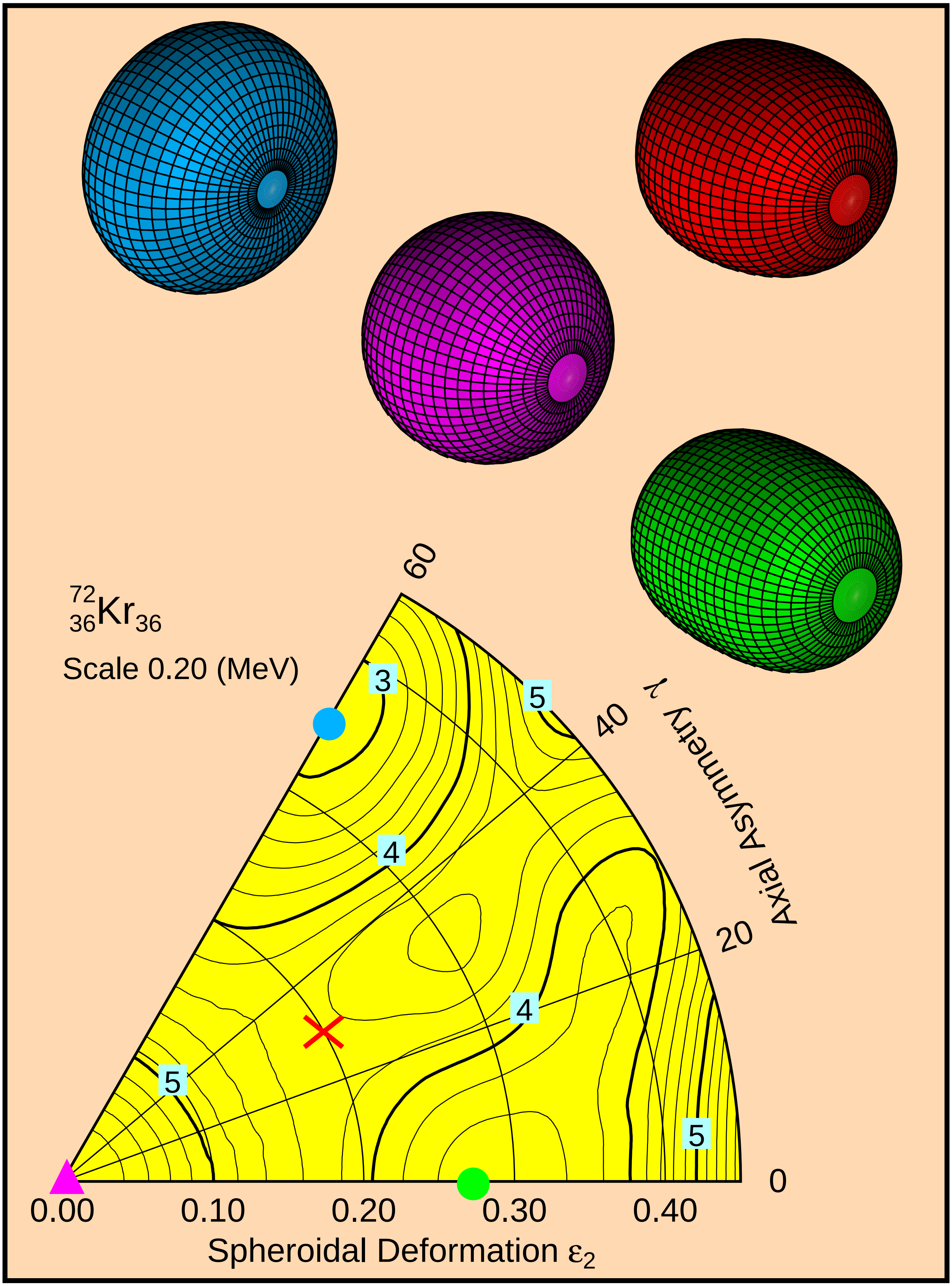

$^{72}_{36}Kr_{36}$
Scale 0.20 (MeV)
60
40
20
0
Axial Asymmetry γ
3
4
5
4
5
5
0.00
0.10
0.20
0.30
0.40
Spheroidal Deformation ε_2

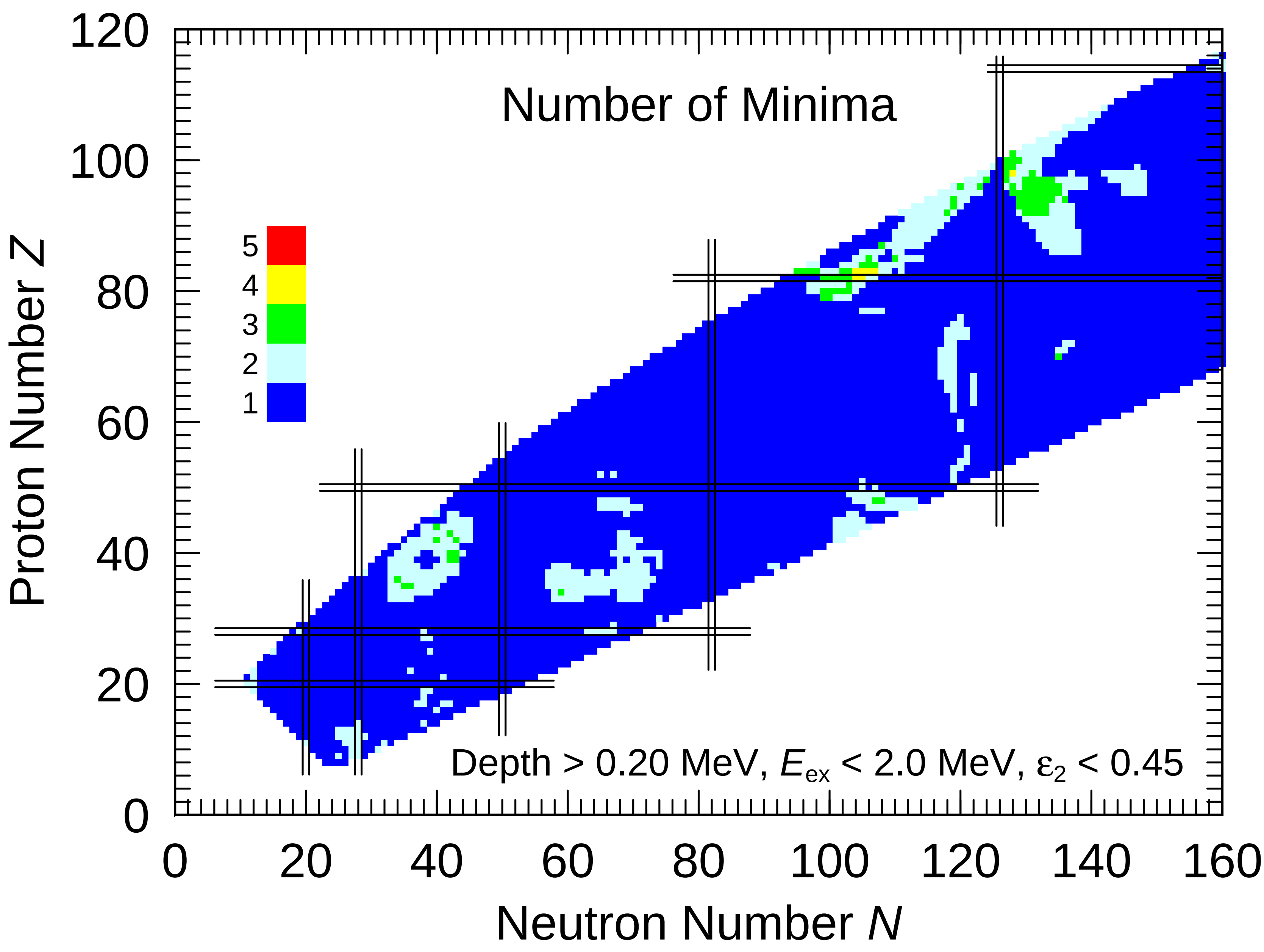

Number of Minima
5
4
3
2
1
Depth > 0.20 MeV, E_{ex} < 2.0 MeV, ε_2 < 0.45
Proton Number Z
Neutron Number N
0
20
40
60
80
100
120
140
160

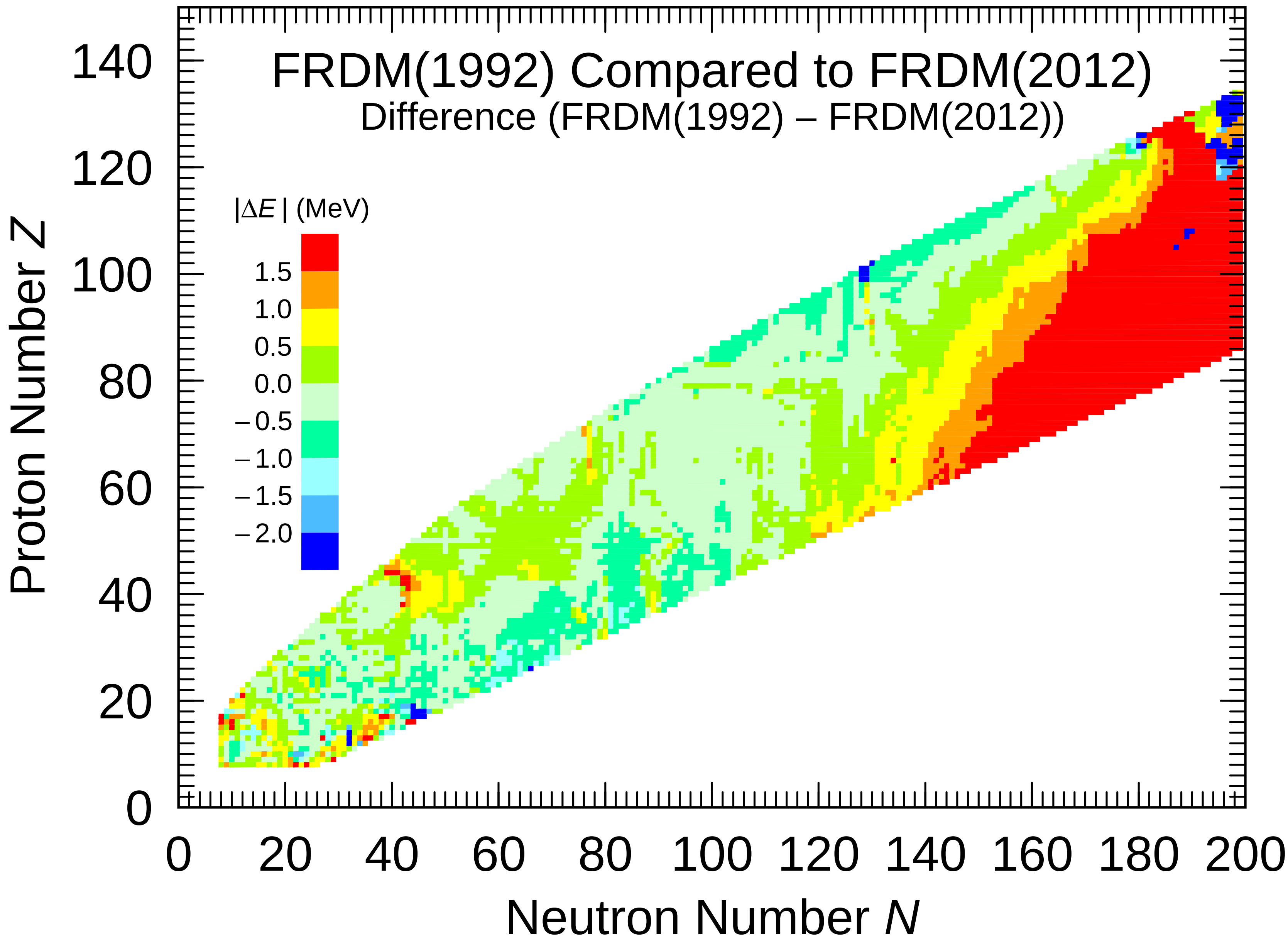
FRDM(1992) Compared to FRDM(2012)
Difference (FRDM(1992) – FRDM(2012))
|ΔE| (MeV)
1.5
1.0
0.5
0.0
−0.5
−1.0
−1.5
−2.0
Proton Number Z
Neutron Number N
0
20
40
60
80
100
120
140
160
180
200

Z	A	AME2003 (MeV)	Trap (MeV)	FRDM(1992) (MeV)	Dev.-1992 (MeV)	FRDM(2012) (MeV)	Dev.-2012 (MeV)
38	80	-70.308	-70.313	-68.840	-1.473	-70.385	0.072
38	81	-71.528	-71.528	-70.650	-0.878	-71.688	0.160
38	84	-80.644	-80.648	-80.880	0.232	-81.474	0.826
40	86	-77.800	-77.971	-77.960	-0.011	-78.646	0.675
41	85	-67.150	-66.279	-65.350	-0.929	-66.559	0.280
42	85	-59.100#	-57.510	-55.750	-1.760	-57.441	-0.069
42	86	-64.560	-64.110	-62.720	-1.390	-63.913	-0.197
42	87	-67.690	-66.882	-66.030	-0.852	-67.043	0.161
43	87	-59.120#	-57.690	-56.540	-1.150	-57.786	0.096

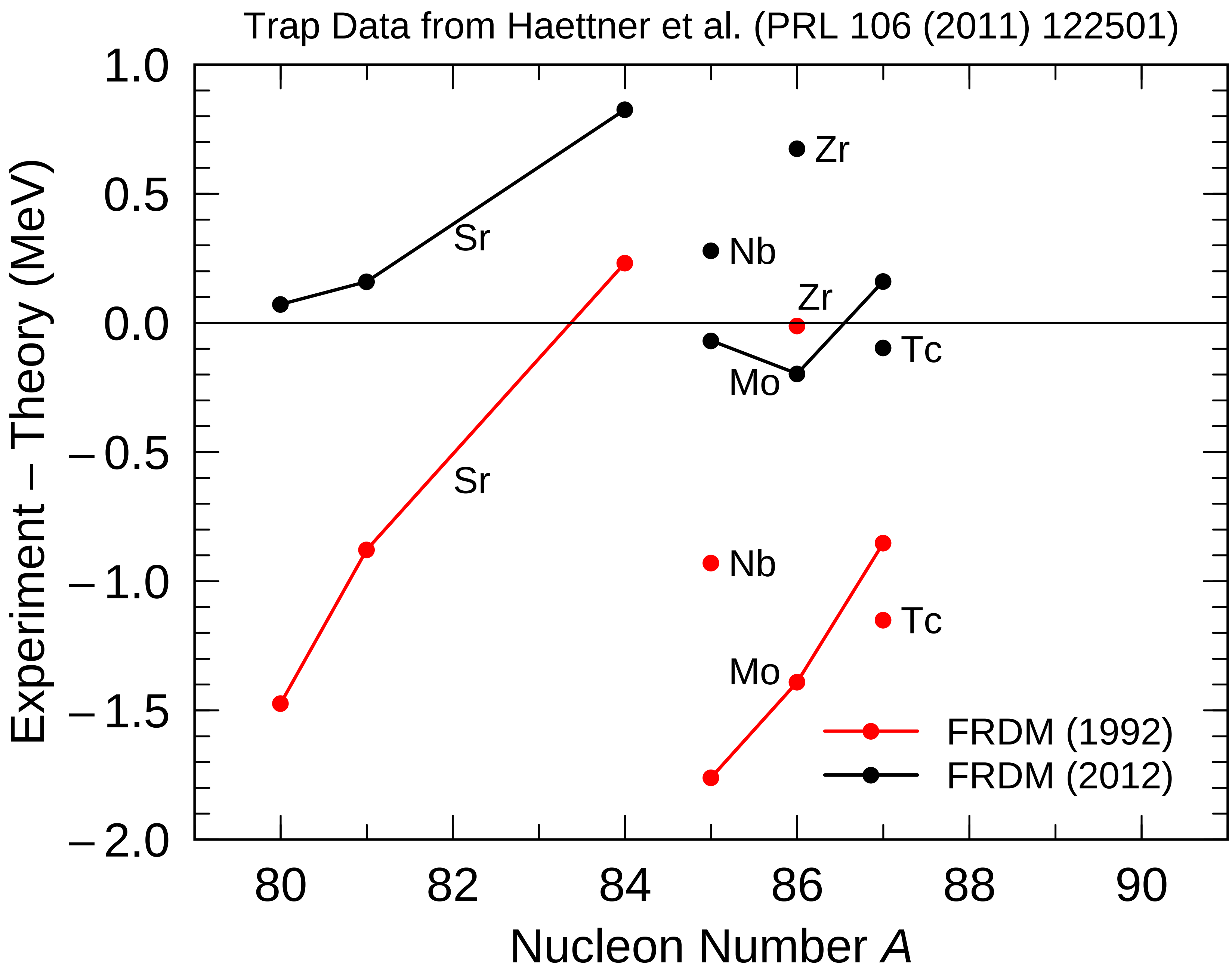

Trap Data from Haettner et al. (PRL 106 (2011) 122501)
1.0
0.5
0.0
−0.5
−1.0
−1.5
−2.0
Experiment – Theory (MeV)
80
82
84
86
88
90
Nucleon Number A
Sr
Zr
Nb
Zr
Tc
Mo
Sr
Nb
Tc
Mo
FRDM (1992)
FRDM (2012)

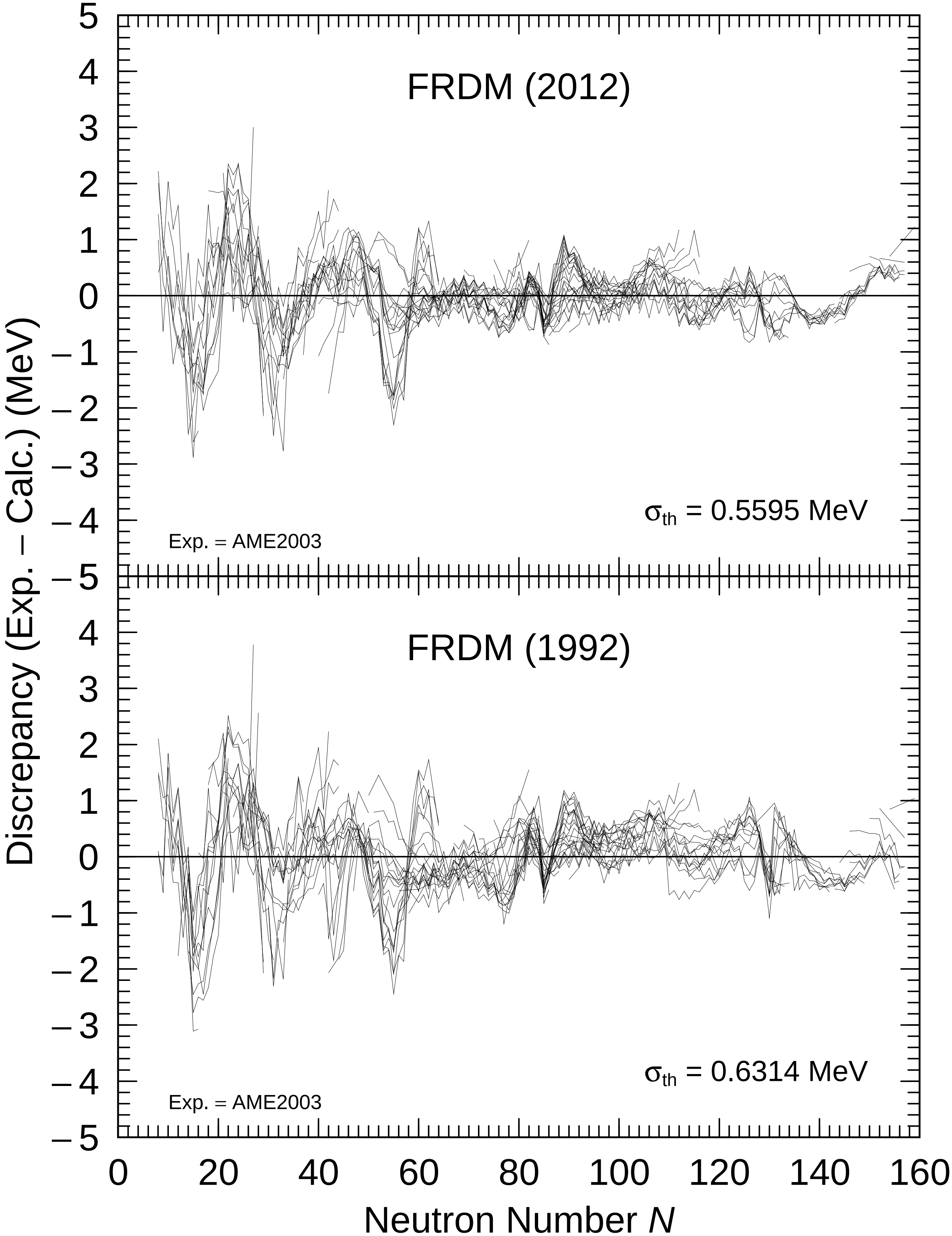
FRDM (2012)
σth = 0.5595 MeV
Exp. = AME2003
FRDM (1992)
σth = 0.6314 MeV
Exp. = AME2003
Discrepancy (Exp. − Calc.) (MeV)
Neutron Number N

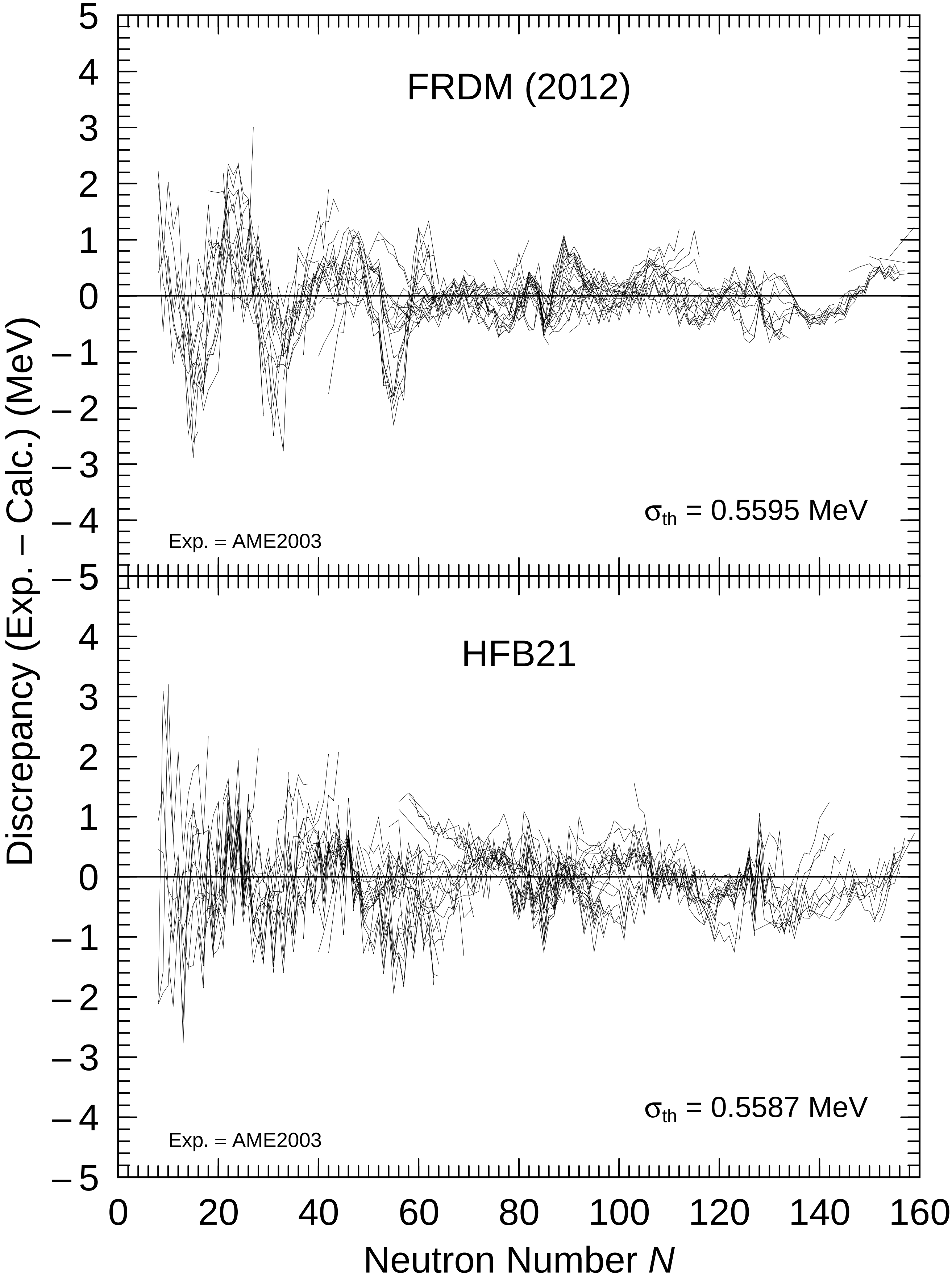
FRDM (2012)
σth = 0.5595 MeV
Exp. = AME2003
HFB21
σth = 0.5587 MeV
Exp. = AME2003
Discrepancy (Exp. − Calc.) (MeV)
Neutron Number N
5
4
3
2
1
0
−1
−2
−3
−4
−5
0
20
40
60
80
100
120
140
160

Q_α Deviations beyond $N = 126$

Region	Model	Nuclei	RMS (MeV)
$Z > 82$	SkM*	46	2.6
$Z > 82$	Sly4	46	2.6
$Z > 82$	HFB21	145	0.409
$Z > 82$	FRDM(1992)	145	0.463
$Z > 82$	FRDM(2012)	145	0.326
$Z > 88$	SkM*	36	1.7
$Z > 88$	Sly4	36	2.2
$Z > 88$	HFB21	101	0.367
$Z > 88$	FRDM(1992)	101	0.448
$Z > 88$	FRDM(2012)	101	0.274

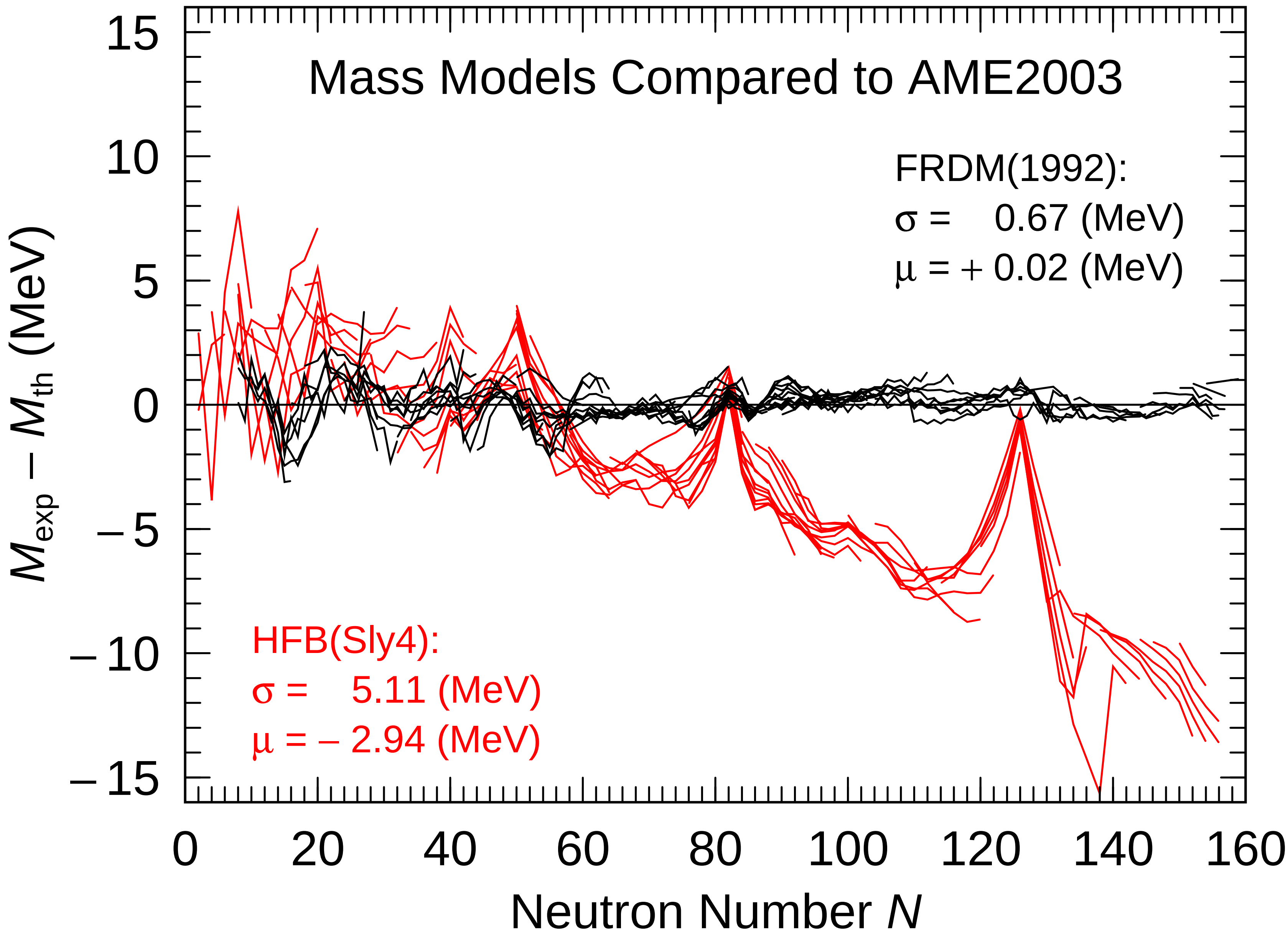

Mass Models Compared to AME2003
FRDM(1992):
σ = 0.67 (MeV)
μ = + 0.02 (MeV)
HFB(Sly4):
σ = 5.11 (MeV)
μ = – 2.94 (MeV)
$M_{exp} - M_{th}$ (MeV)
Neutron Number N
15
10
5
0
– 5
– 10
– 15
0
20
40
60
80
100
120
140
160

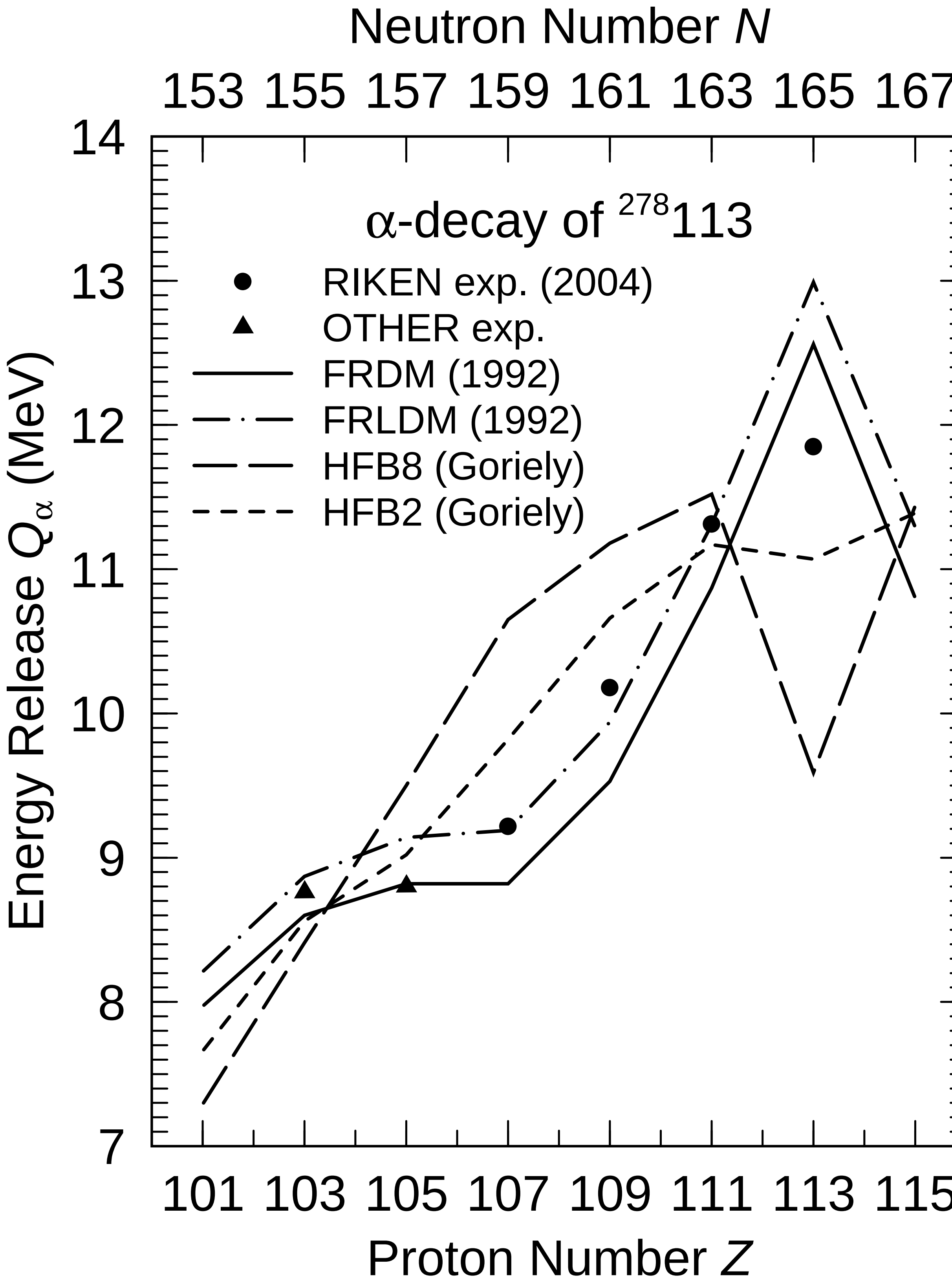

Neutron Number N
153 155 157 159 161 163 165 167
α-decay of 278113
RIKEN exp. (2004)
OTHER exp.
FRDM (1992)
FRLDM (1992)
HFB8 (Goriely)
HFB2 (Goriely)
Energy Release Qα (MeV)
7 8 9 10 11 12 13 14
101 103 105 107 109 111 113 115
Proton Number Z

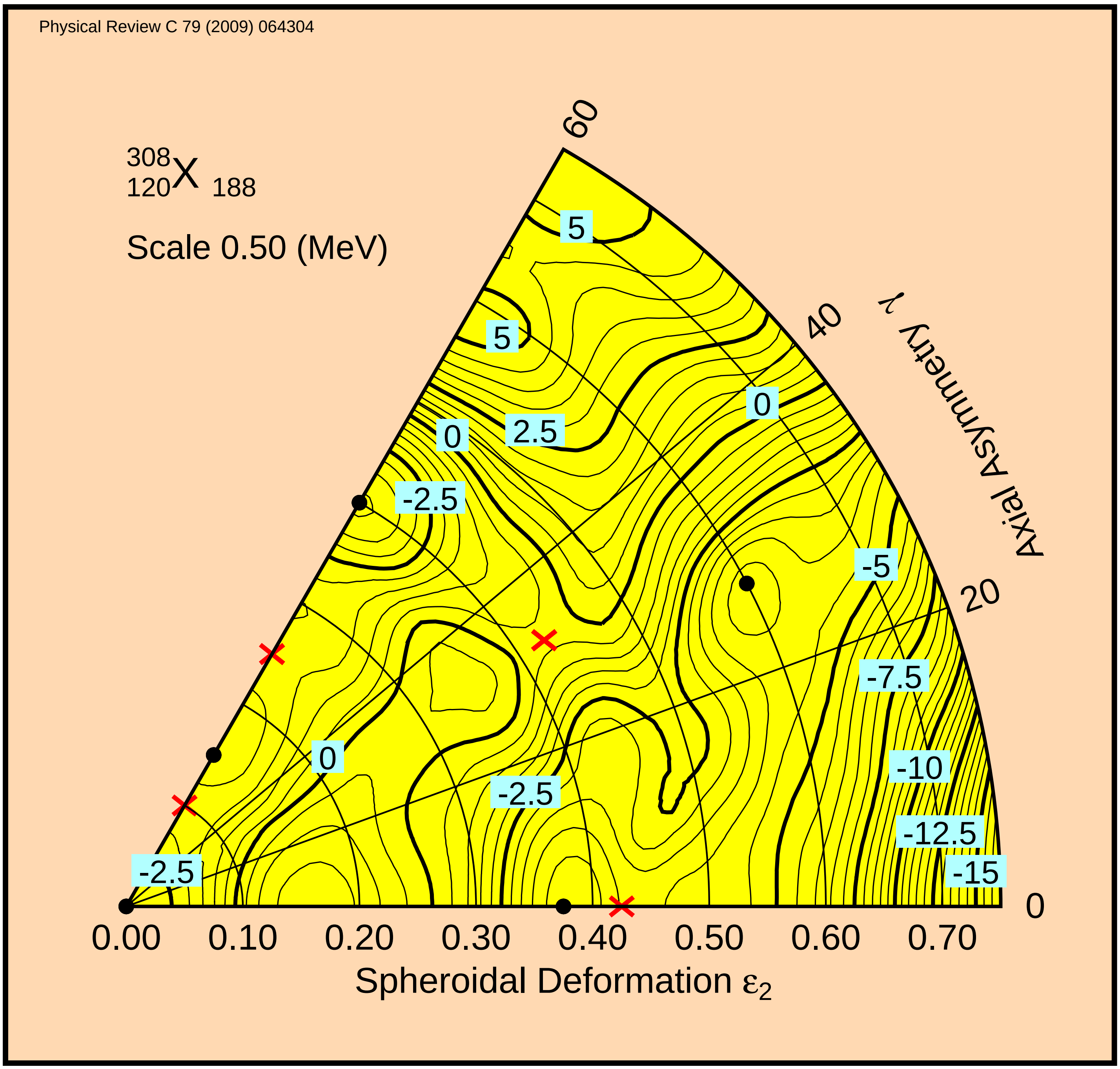

Physical Review C 79 (2009) 064304
308
120
X
188
Scale 0.50 (MeV)
60
40
20
0
Axial Asymmetry γ
5
5
2.5
0
0
-2.5
-5
-7.5
0
-10
-2.5
-12.5
-2.5
-15
0.00
0.10
0.20
0.30
0.40
0.50
0.60
0.70
Spheroidal Deformation ε2

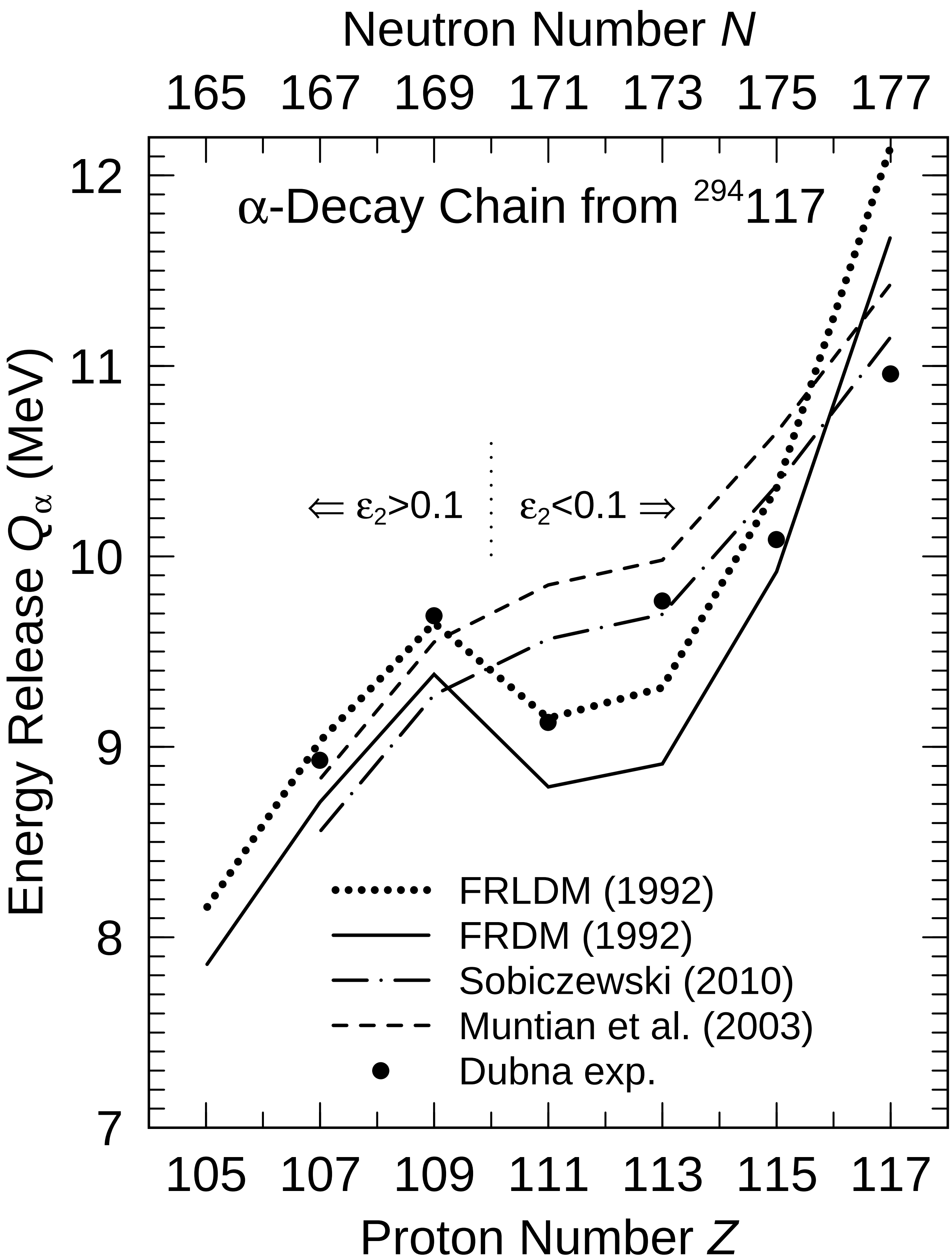
Neutron Number N
165 167 169 171 173 175 177
α-Decay Chain from 294117
⇐ ε2>0.1
ε2<0.1 ⇒
Energy Release Qα (MeV)
12
11
10
9
8
7
FRLDM (1992)
FRDM (1992)
Sobiczewski (2010)
Muntian et al. (2003)
Dubna exp.
105 107 109 111 113 115 117
Proton Number Z

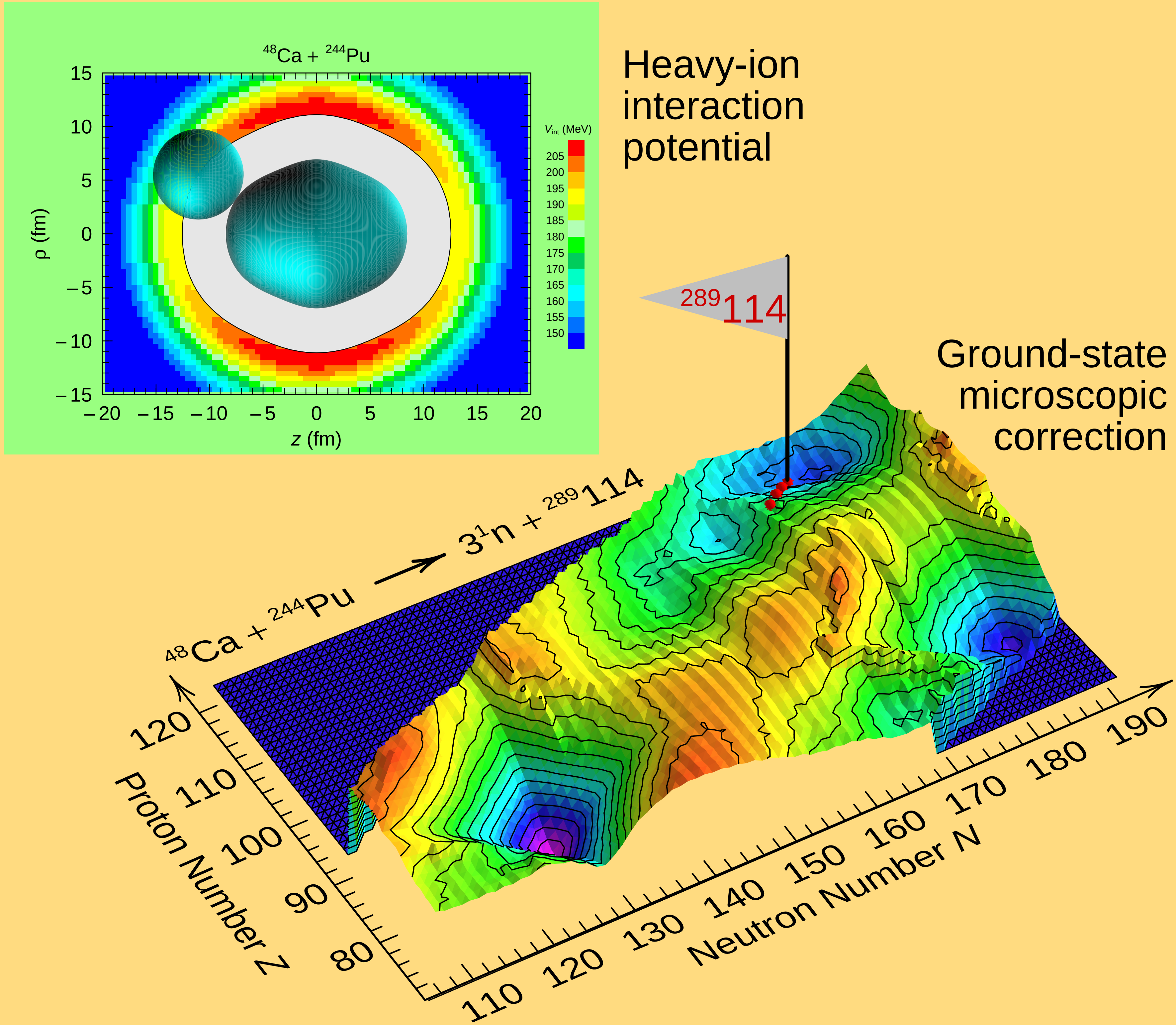

Heavy-ion interaction potential
$^{48}Ca + ^{244}Pu$
V_{int} (MeV)
205
200
195
190
185
180
175
170
165
160
155
150
ρ (fm)
z (fm)
$^{289}114$
Ground-state microscopic correction
$^{48}Ca + ^{244}Pu \rightarrow 3\,^{1}n + ^{289}114$
Proton Number Z
Neutron Number N

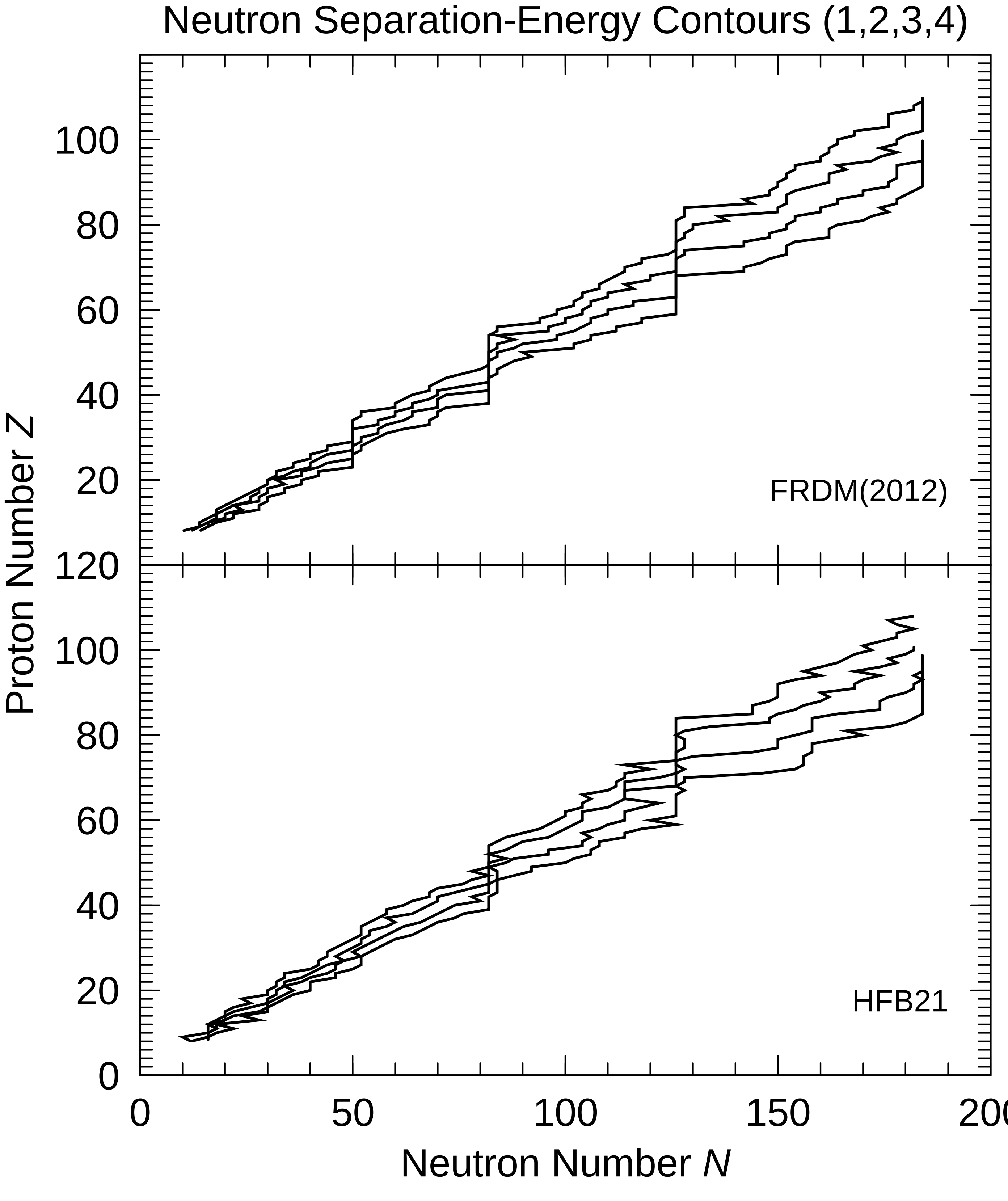

Neutron Separation-Energy Contours (1,2,3,4)
Proton Number Z
Neutron Number N
FRDM(2012)
HFB21
0
20
40
60
80
100
120
50
150
200

I N T E R M I S S I O N

then

F I S S I O N

Five Essential Fission Shape Coordinates

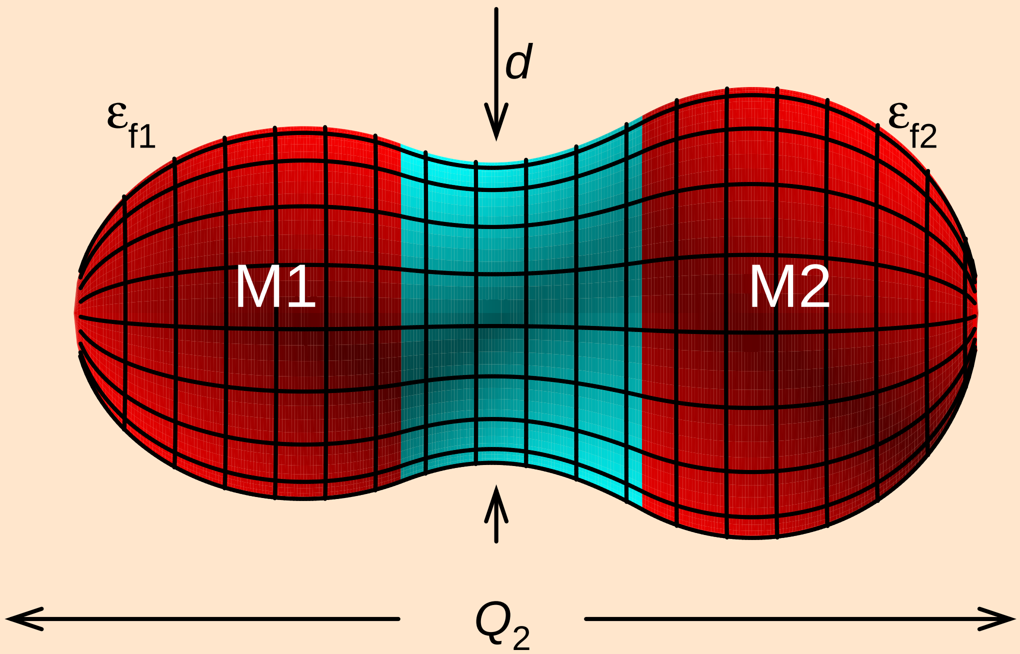

45	Q_2	~	Elongation (fission direction)
$\otimes$			
35	α_g	~	(M1-M2)/(M1+M2) Mass asymmetry
$\otimes$			
15	ε_{f1}	~	Left fragment deformation
$\otimes$			
15	ε_{f2}	~	Right fragment deformation
$\otimes$			
15	d	~	Neck

$\Rightarrow$ 5 315 625 grid points – 306 300 unphysical points

$\Rightarrow$ 5 009 325 physical grid points

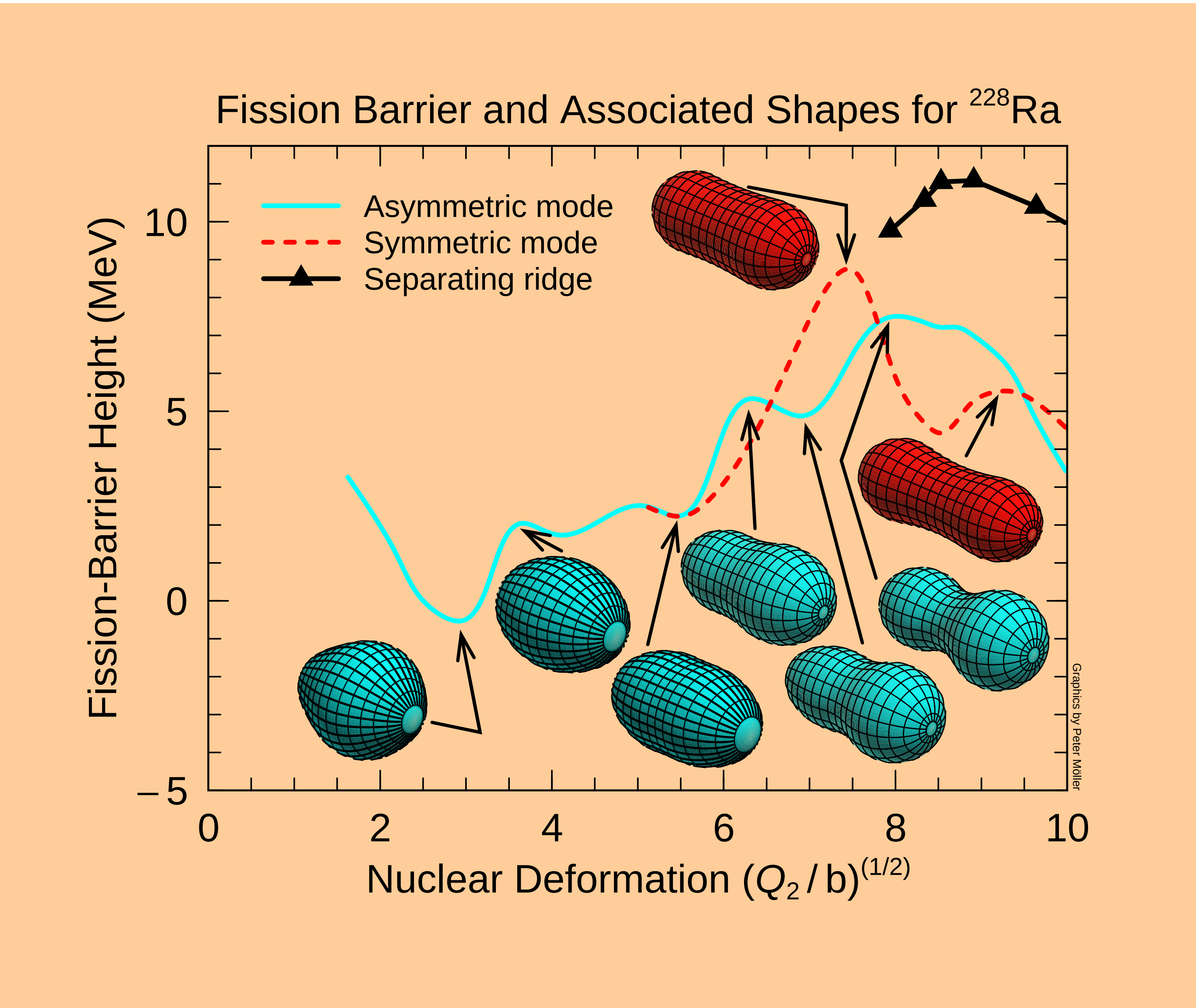

Fission Barrier and Associated Shapes for 228Ra
Asymmetric mode
Symmetric mode
Separating ridge
Fission-Barrier Height (MeV)
10
5
0
−5
0
2
4
6
8
10
Nuclear Deformation (Q2 / b)(1/2)
Graphics by Peter Möller

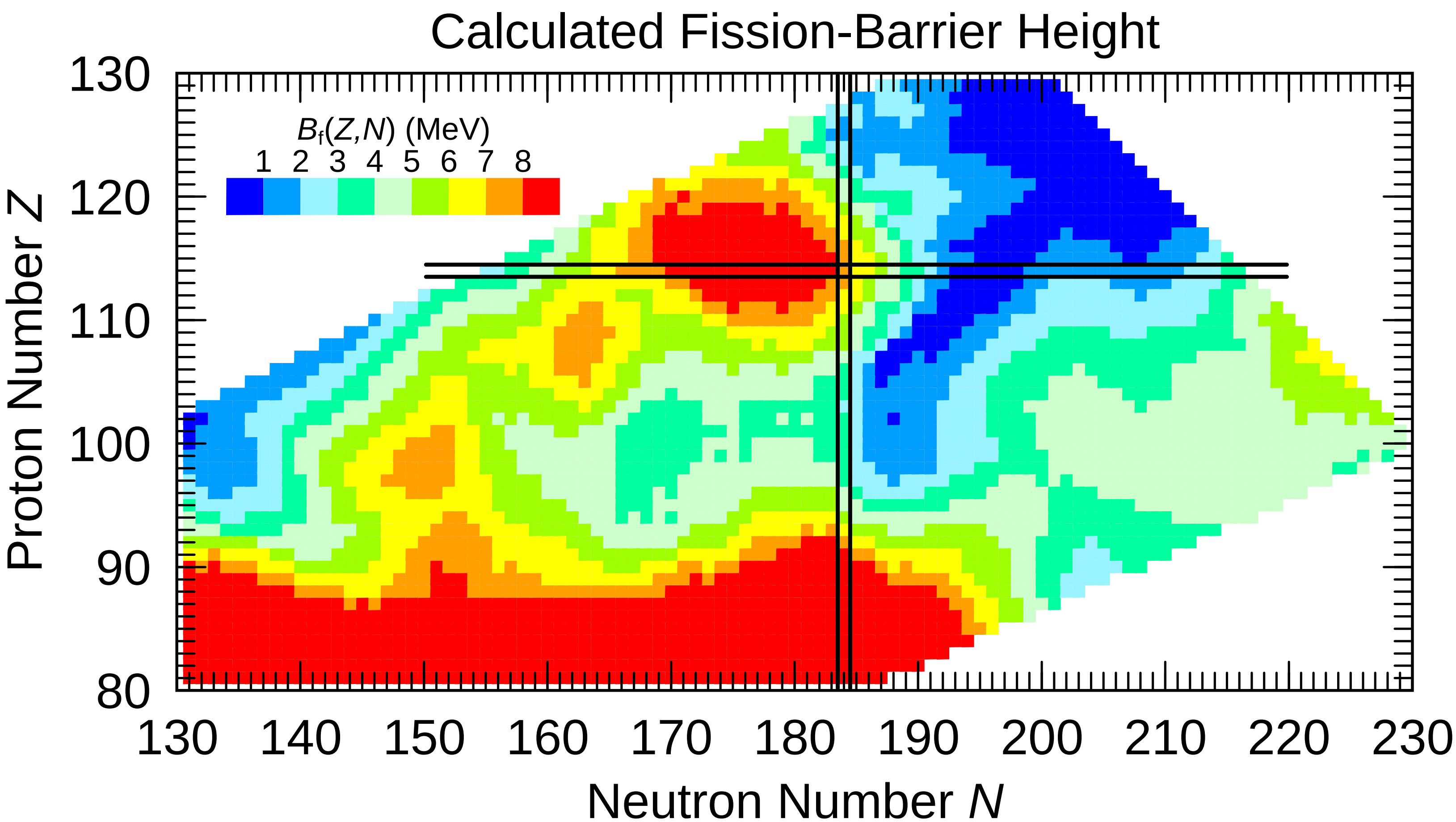

Calculated Fission-Barrier Height
$B_f(Z,N)$ (MeV)
1 2 3 4 5 6 7 8
130
120
110
100
90
80
Proton Number Z
130 140 150 160 170 180 190 200 210 220 230
Neutron Number N

Deficiencies and improvements to fits to $N_{r,☼}$

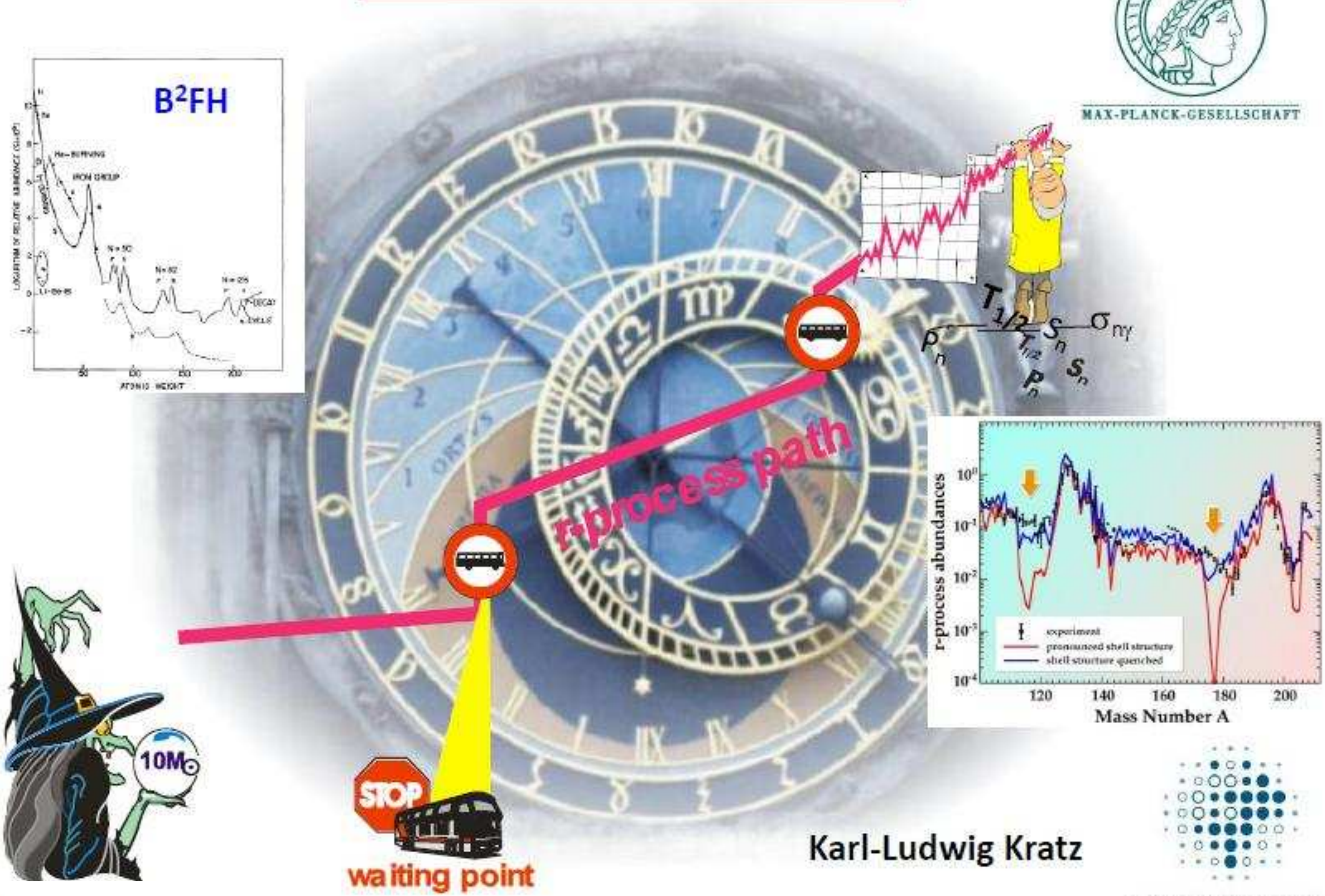

Karl-Ludwig Kratz

Rußbach, 2014

The FK²L waiting-point approach (IV)

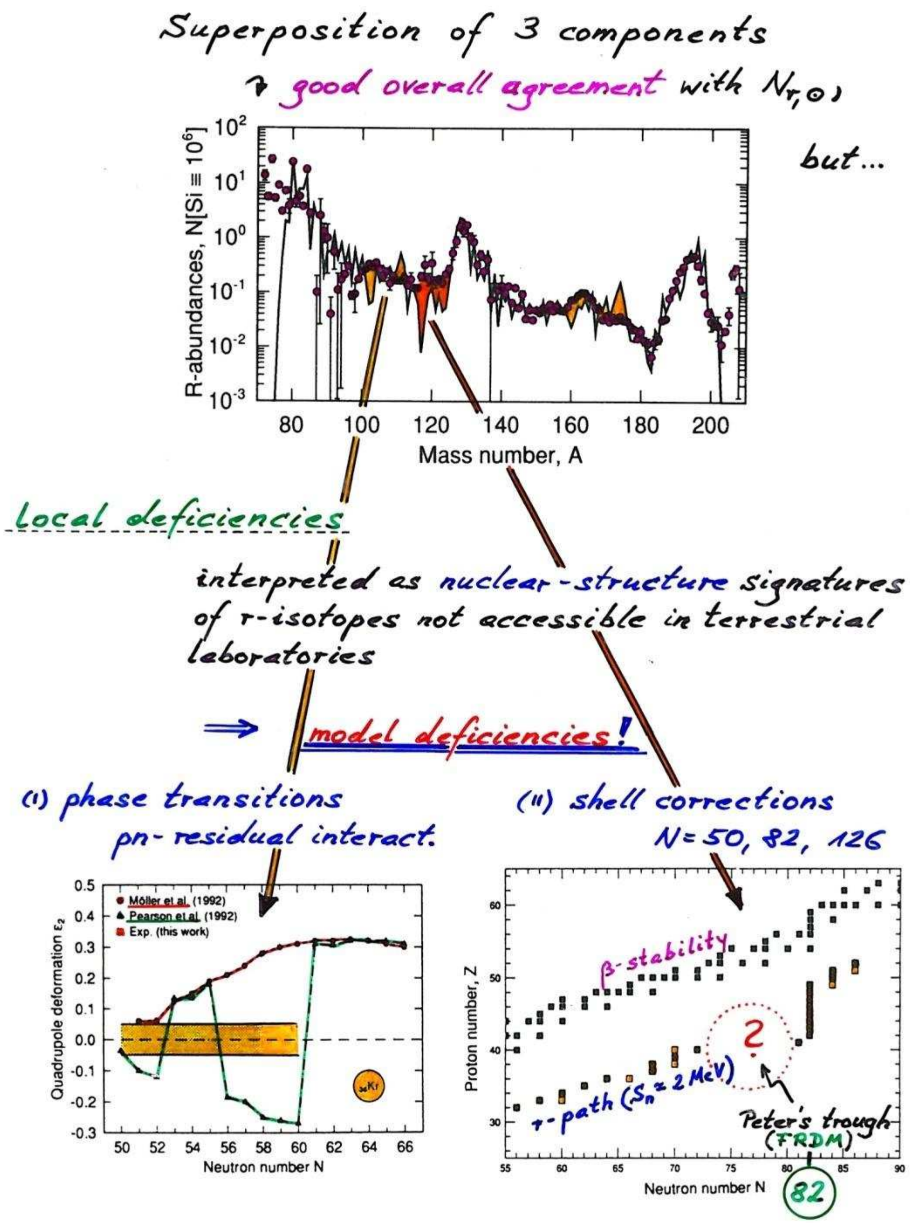

"...best fit so far...;
long-standing problem solved..."
W. Hillebrandt

"...call for a deeper study...
before rushing into numerical results...
and premature comparisons with the observed abundances"
M. Arnould

birth of N=82
"shell-quenching"
idea ...

...this catchword coined by W. Nazarewicz later led to semantics and misinterpretations

Impact of nuclear masses at N = 82

Already FK²L (ApJ 403) concluded from their fits to $N_{r,\odot}$:

"the calculated r-abundance "trough" in the A ≈ 120 region reflects the weakening of the shell strength below $^{132}Sn_{82}$."

Effect of S_n around N=82 shell closure

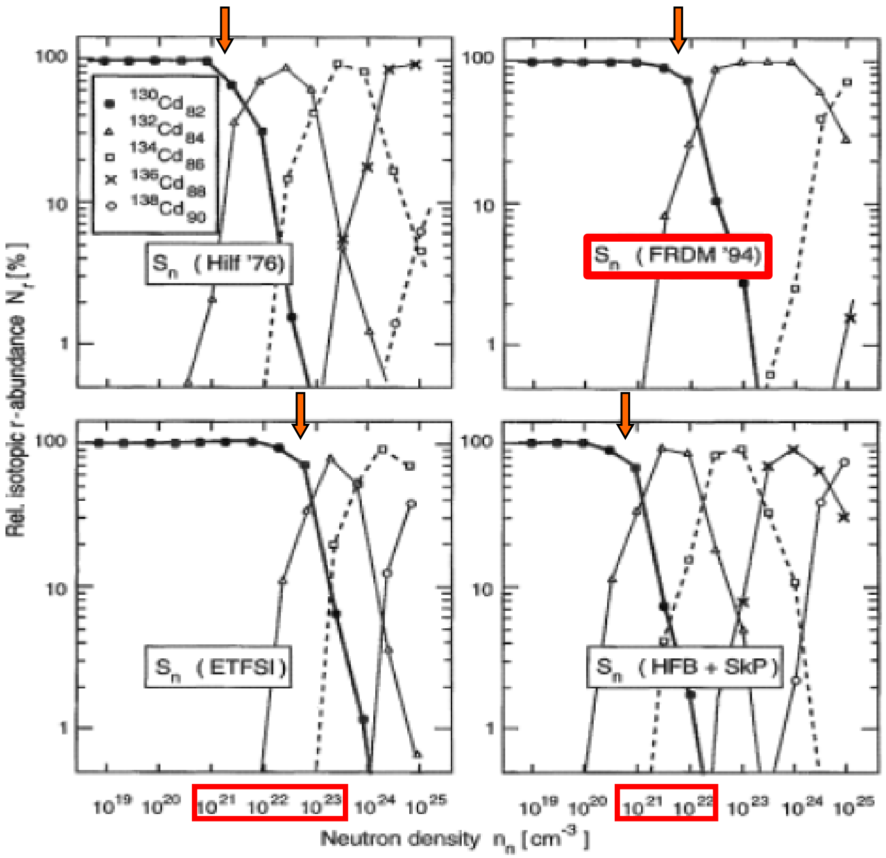

astrophys. parameters (T_9, n_n, τ_n) and $T_{1/2}$ kept constant

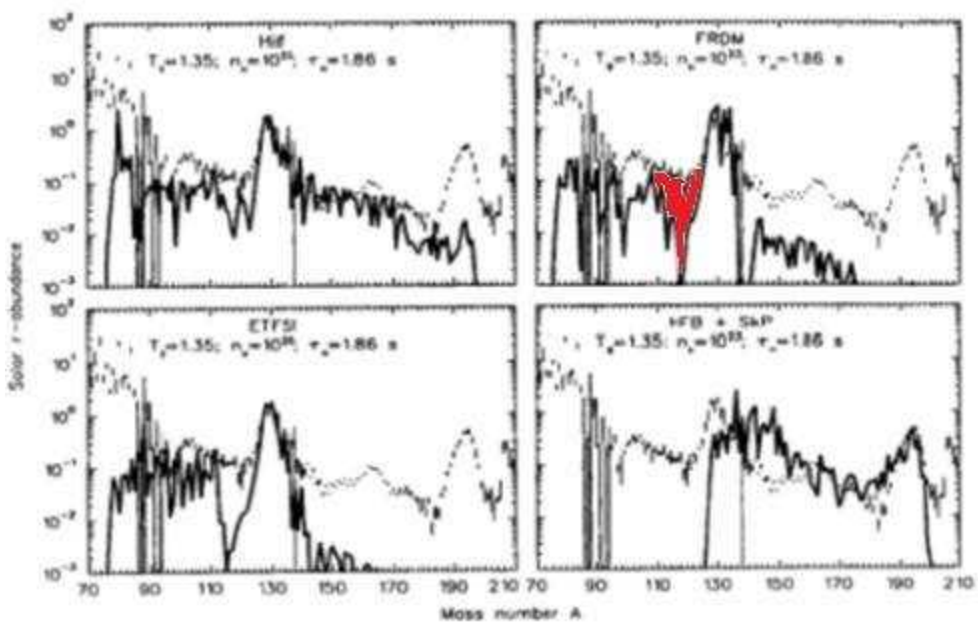

"static" calculations (Saha equation)
⟹ break-out at N=82 ^{130}Cd

"time-dependent" calculations (w.-p.)
⟹ r-matter flow to and beyond A=130

N=82 „shell-quenching“

Phys. Lett. B355, 37 (1995)

Influence of shell-quenching far from stability on the astrophysical r-process

B. Chen [a], J. Dobaczewski [b], K.-L. Kratz [c], K. Langanke [a], B. Pfeiffer [c], F.-K. Thielemann [d], P. Vogel [e]

Use spherical **HFB/SkP** mass model ⇨ **FRDM+HFB/SkP** “hybrid model” around N=82

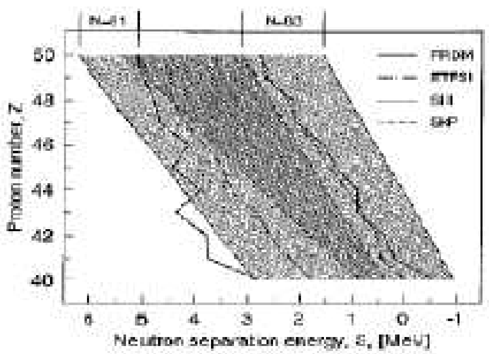

ΔS_n as a measure of the N=82 shell strength

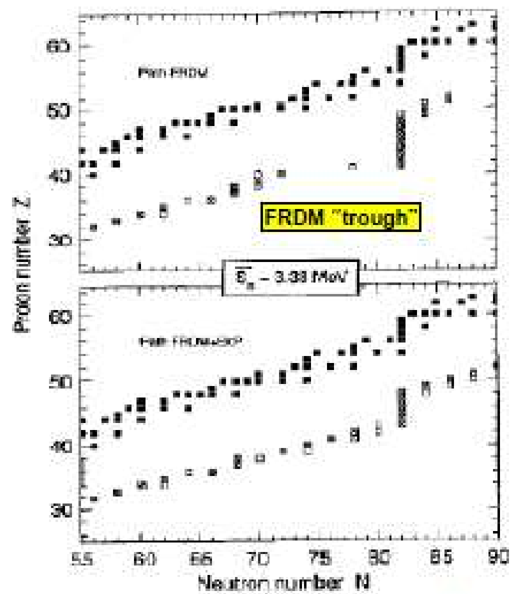

population of r-path

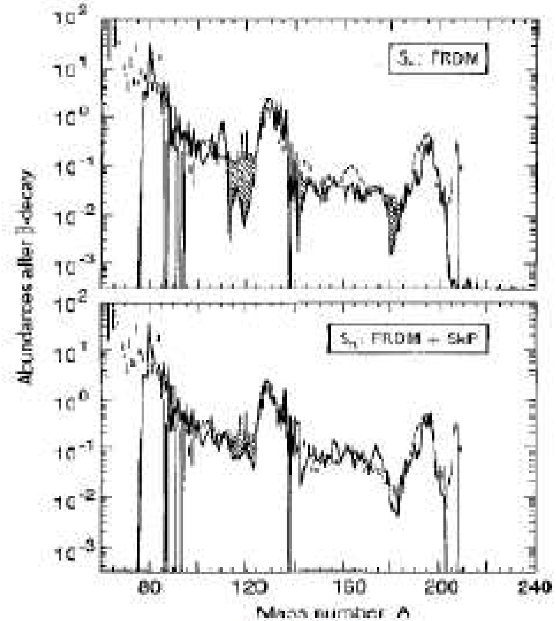

$N_{r,\odot}$ fits

Effects of N=82 "shell quenching"

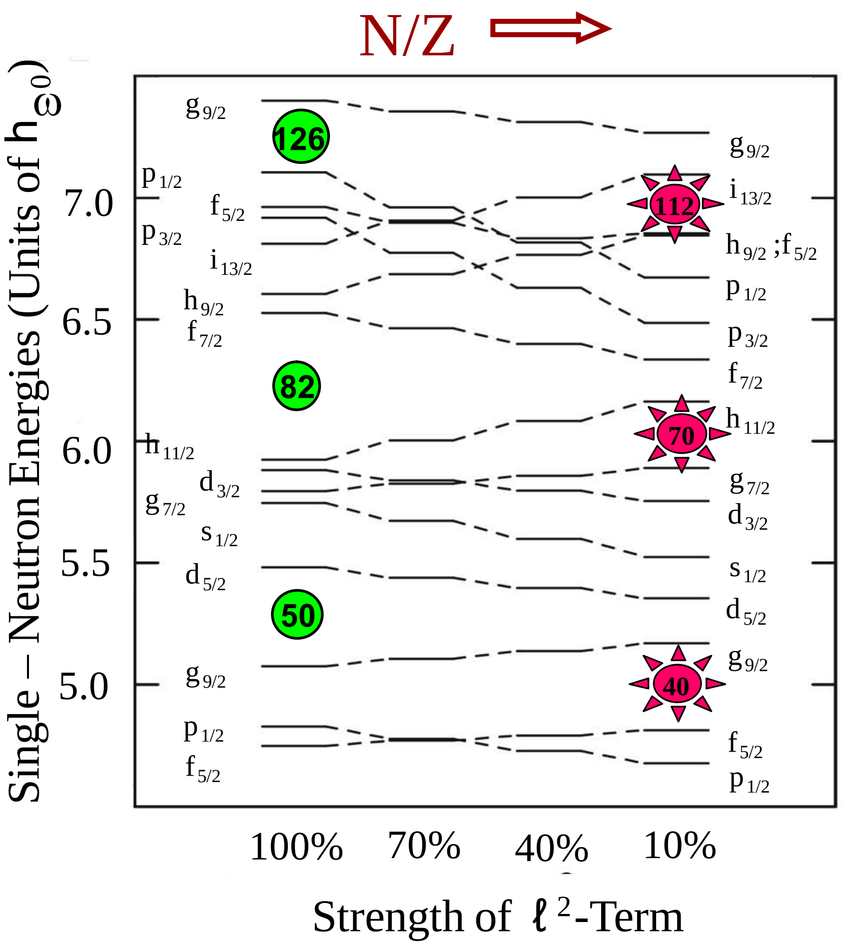

B. Pfeiffer et al.,
Acta Phys. Polon. **B27** (1996)

"Shell quenching"

…reduction of the spin-orbit coupling strength;
caused by strong interaction between bound and continuum states;
due to diffuseness of "neutron-skin" and its influence on the central potential…

- high-j orbitals ⇑ (e.g. $\nu h_{11/2}$)
- low-j orbitals ⇓ (e.g. $\nu d_{3/2}$)
- evtl. crossing of orbitals
- new “magic” numbers / shell gaps (e.g. $^{110}Zr_{70}$, $^{170}Ce_{112}$)

change of

- shell-gaps
- deformation
- r-process path (S_n)
- r-matter flow (τ_n)

r-Process calculations with MHD-SN models

2012 … new "hot r-process topic" ➔ **magnetohydrodynamic SNe**
… but, unfortunately not with the optimum nuclear-physics input…

Phys.Rev. C85 (2012)

Impact of new β-decay half-lives on r-process nucleosynthesis

Nobuya Nishimura,[1,2,*] Toshitaka Kajino,[3,4] Grant J. Mathews,[5] Shunji Nishimura,[6] and Toshio Suzuki[7]

"We investigate the effect of newly measured ß-decay half-lives on r-process nucleosynthesis. We adopt … a magnetohydrodynamic supernova explosion model… The ($T_{1/2}$) effect slightly alleviates, but does not fully explain, the tendency of r-process models to underproduce isotopes with A = 110 – 120…"

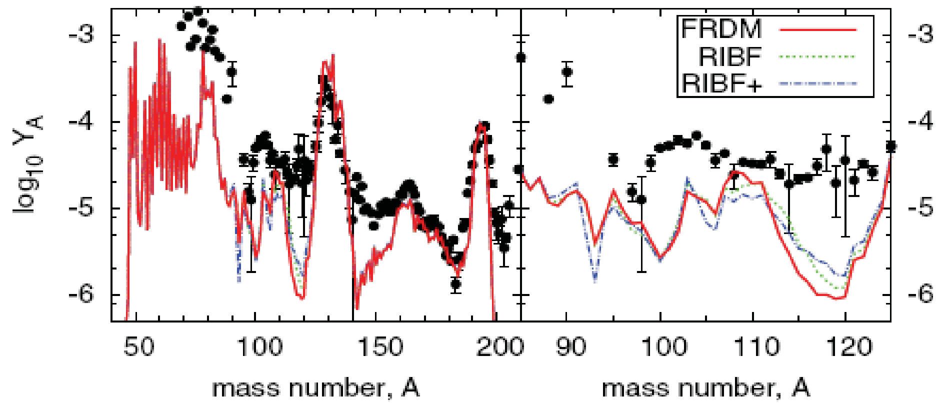

In both cases FRDM 1992 masses have been used
partly misleading conclusions

Ap.J. Letter 750 (2012)

MAGNETOROTATIONALLY DRIVEN SUPERNOVAE AS THE ORIGIN OF EARLY GALAXY r-PROCESS ELEMENTS?

C. Winteler[1], R. Käppeli[2], A. Perego[1], A. Arcones[3,4], N. Vasset[1], N. Nishimura[1], M. Liebendörfer[1], and F.-K. Thielemann[1]

"We examine magnetohydrodynamically driven SNe as sources of r-process elements in the early Galaxy… … the formation of bipolar jets could naturally provide a site for the strong r-process…"

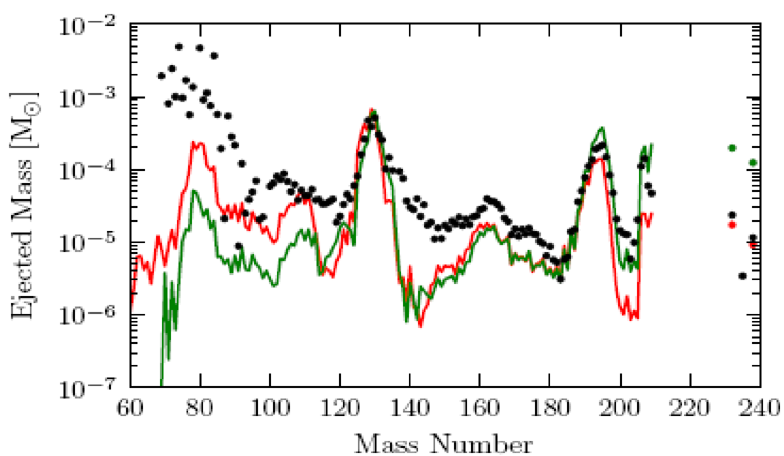

Deviation from SS-r: FRDM vs. ETFSI-Q

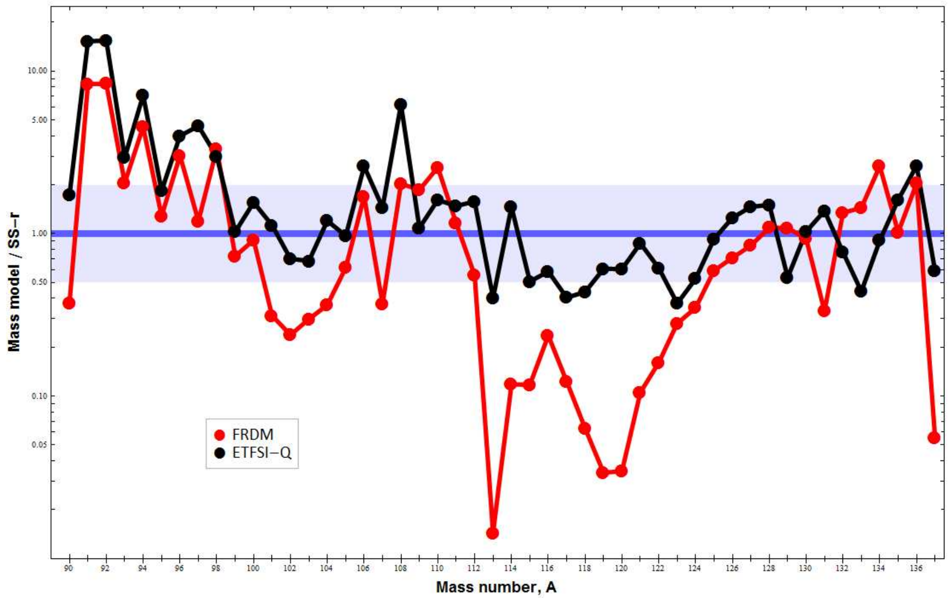

How to fill up the FRDM A ≈ 115 "trough" ?

- if via $T_{1/2}$ (as e.g. suggested by Nishimura, Kajino et al.; PRC 85 (2012)), on average all r-progenitors between ^{110}Zr and ^{126}Pd should have
  7.5 x $T_{1/2}$(FRDM) ≈ 350 ms →
  2 x $T_{1/2}$(^{130}Cd) at top of r-peak
- it **must** be the progenitor masses, via S_n (and correlated deformation ε_2)

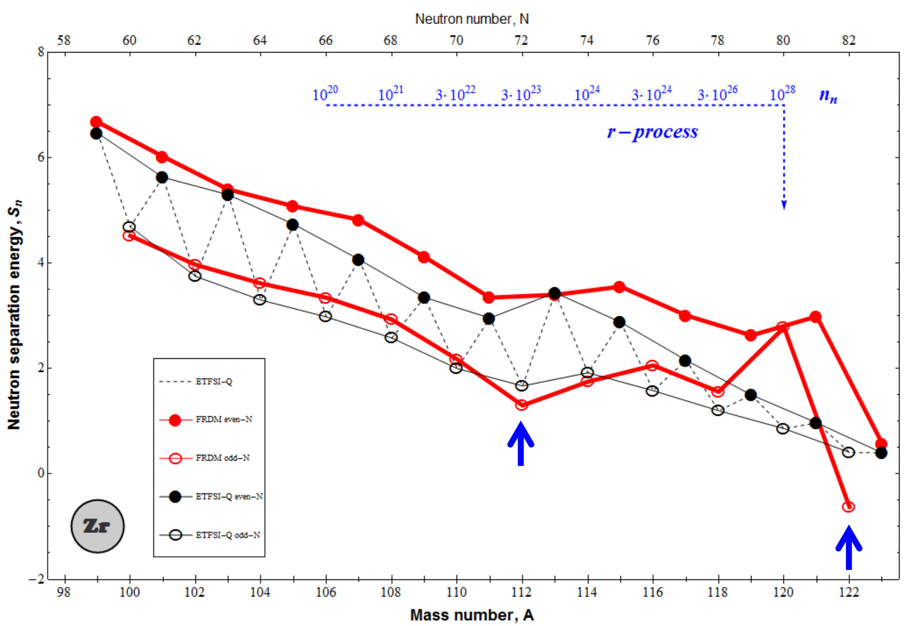

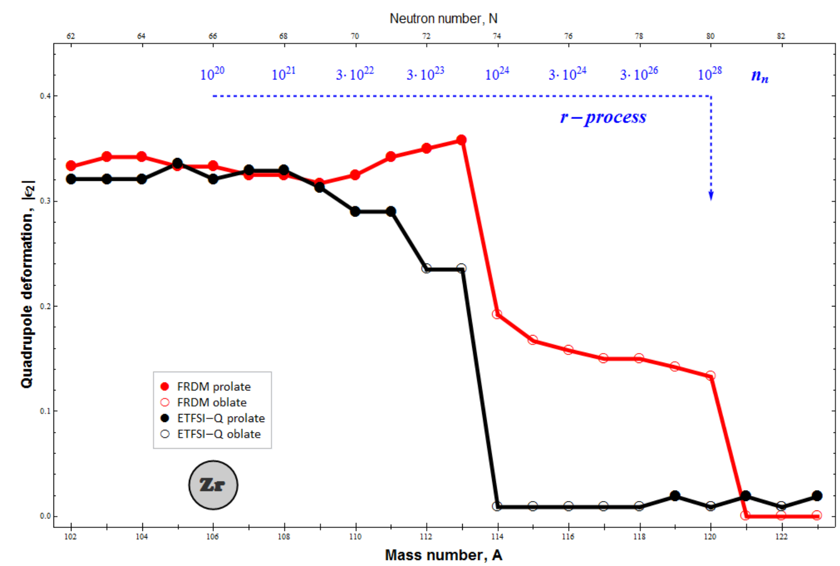

Reproduction of $N_{r,\odot}$

Superposition of S-components with **Y_e=0.45**;

weighting according to Y_{seed}

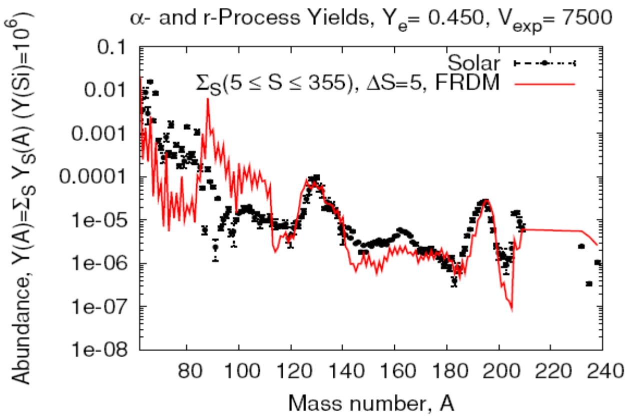

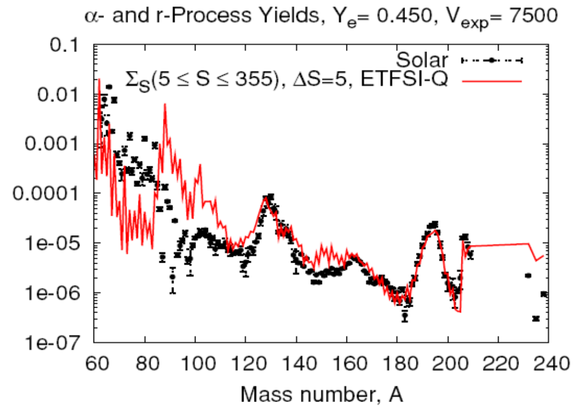

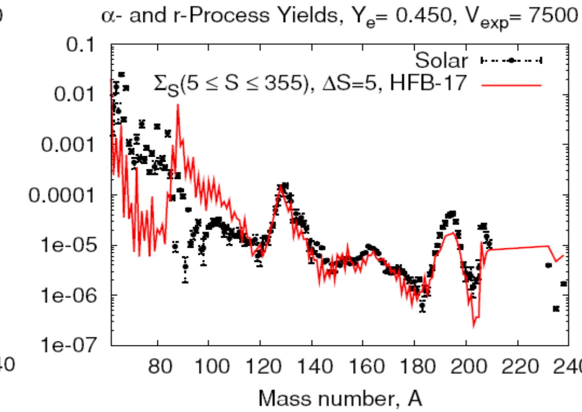

No exponential fit to $N_{r,\odot}$!

Entropy S	Process duration [ms] FRDM	ETFSI-Q	Remarks
150	54	57	A≈115 region
180	**209**	**116**	**top of A≈130 peak**
220	422	233	REE pygmy peak
245	**691**	**339**	**top of A≈195 peak**
260	1290	483	Th, U
280	2280	710	fission recycling
300	4310	1395	" "

⇨ significant effect of **"shell-quenching"** below doubly-magic ^{132}Sn

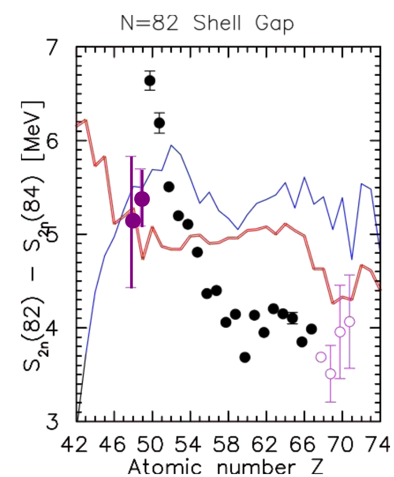

The $N_{r,\odot}$ rare-earth pygmy peak

What is the origin of the REE r-abundance peak ?

Already about 15 years ago,
first indications from calculations
using two different mass models
⇨ effect of **S_n**

SPHERICAL **DEFORMED**

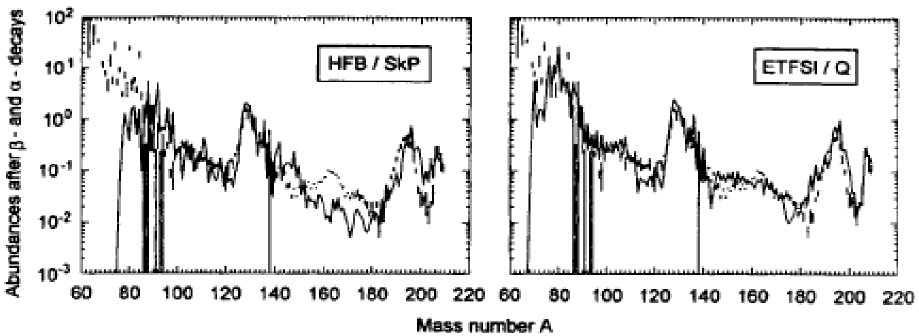

Today, in principle confirmed by
new calculations using the
“deformed“ FRDM 2012 and
two different $T_{1/2}$ & P_n data sets
⇨ effect of **β-decay properties**

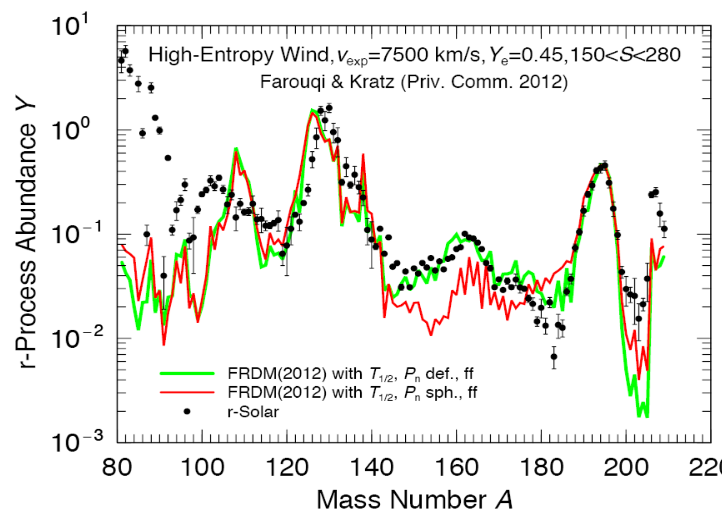

REE pygmy peak due to **deformation**, not from fission cycling!

First HEW calculations with FRDM(2012) and QRPA(2012)

Good news at the end…

Comparison between $N_{r,\odot}$ and r-abundances calculated with **FRDM(1992)** and **FRDM(2012)**

in both cases normalized to ^{195}Pt.

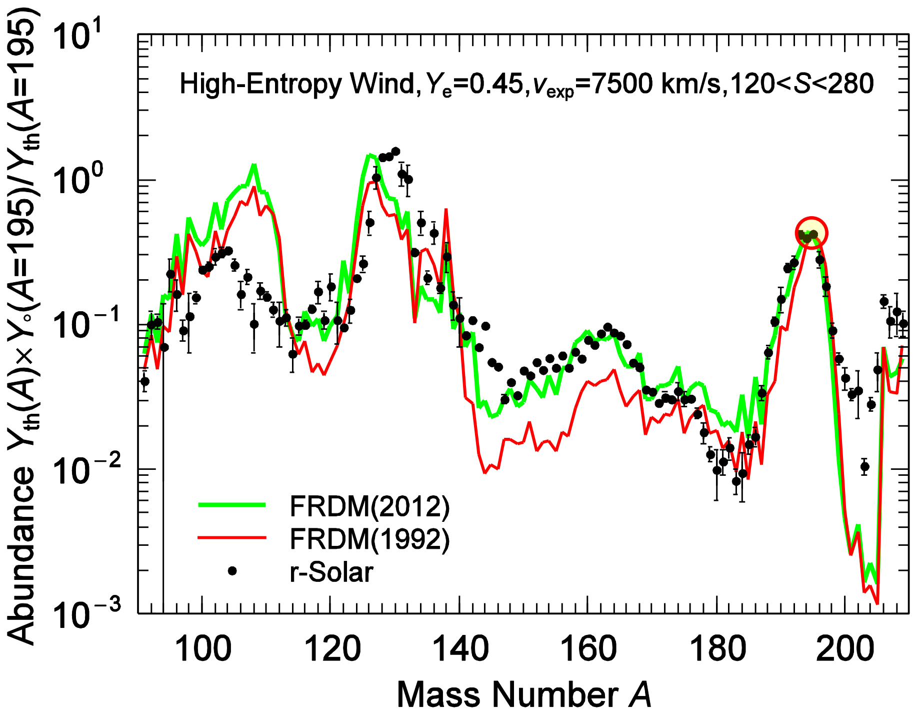

Improvements and remaining deficiencies:

- still overabundances in the 80≤A≤110 mass region
- "abundance trough" at A≈120 removed
- 2nd r-peak slightly improved, but top still too low
- N=82 bottle-neck behavior improved
- perfect reproduction of the deformed REE "pygmy-peak"
- shape of 3rd r-peak well reproduced
- shape-transition region above N=126 still imperfect ⇨ deep trough
- Pb,Bi here too low because major contribution from α-backdecay not yet included

Summary and conclusion:

promising progress, but still much remains to be done in all interrelated fields